Research Square

Preprints are preliminary reports that have not undergone peer review.
They should not be considered conclusive, used to inform clinical practice,
or referenced by the media as validated information.

Mechanical Behavior of Laminated Recycled Tyre Rubber Isolators and Their Effect on the Dynamic Response of a Steel Structure

Syed Abbas Gillani

syedabbasgillani5@gmail.com

Capital University of Science and Technology

Ahmad Ibrahim Alam

Capital University of Science and Technology

Muhammad Ali Haider

Capital University of Science and Technology

Majid Ali

Capital University of Science and Technology

Research Article

Keywords: Base Isolation, Blast Loading, Free Vibration, Harmonic Loading, High Damping Rubber Bearing, Pushover Test, Steel Structures, Tyres, Waste Rubber

Posted Date: November 27th, 2026

DOI: https://doi.org/10.21203/rs.3.rs-11867551/v1

License: This work is licensed under a Creative Commons Attribution 4.0 International License.
Read Full License

Additional Declarations: No competing interests reported.

Mechanical Behavior of Laminated Recycled Tyre Rubber Isolators and Their Effect on the Dynamic Response of a Steel Structure

Syed Abbas Gillani[1,*], Ahmad Ibrahim Alam[1], Muhammad Ali Haider[1] and Majid Ali[1]

[1]Department of Civil Engineering, Capital University of Science and Technology, Islamabad, Pakistan

Correspondence: syedabbasgillani5@gmail.com

Abstract: Laminated elastomeric isolators have a high vertical stiffness, low lateral stiffness, and hysteretic damping to decouple a structure from ground motion. They are expensive and require engineered rubber compounds, thus restricting their application to high resource areas. This paper investigates the mechanical behavior of Waste Tyre Rubber Base Isolator (WTRBI). A scaled-down isolator with 22 layers of rubber, each with a thickness of 1 mm, and without any steel shim and lead core, was tested under compression and lateral pushover. A one-storey, one-bay 1/20th scale steel frame was then subjected to static pushover, free vibration, impact and shake-table loading. The load carried by the isolator was found to have a vertical stiffness of 0.391 kN/mm and an effective lateral stiffness of 0.891 N/mm. It has a Poisson's ratio of 0.48 which means it has near incompressible behavior. The lateral stiffness of the isolated structure was reduced by 63.8% and the fundamental period of the isolated structure increased from 0.13 s to 0.31 s. For harmonic excitation, the acceleration in response was reduced by approximately 30% and the base shear was reduced by approximately 29.6%. The hysteresis loops increased the equivalent viscous damping from approximately 5.6% to approximately 14% The roof acceleration from the impact tests was approximately 32% less than the base acceleration of the column. These findings demonstrate that recycled tyre rubber can serve as an isolation system, to a certain extent. Further cyclic shear characterization and further constitutive modelling and full-scale validation are required.

Keywords: Base Isolation, Blast Loading, Free Vibration, Harmonic Loading, High Damping Rubber Bearing, Pushover Test, Steel Structures, Tyres, Waste Rubber.

1. Introduction

Seismic design practices nowadays are based on making structures stiffer and stronger. This increases force requirements and causes damage to structures under severe earthquakes. Seismic base isolation separates the superstructure from the ground by a layer which resists movement in the vertical direction but is compliant in the horizontal direction. This increases the fundamental period, dissipates energy and decreases the seismic energy transferred to the structure (Ragni et al., 2026; Razavian Amrei et al., 2026; Yang et al., 2026; Zelleke & Matsagar, 2026; H.-T. Zhang et al., 2026). Leading research by various authors (Gallardo et al., 2026; Pratama & Ariani, 2026; Solgi et al., 2025; Wahab & Zhong, 2026; Xiang et al., 2026; J. Zhang et al., 2026) has demonstrated that isolation systems, including lead rubber bearings (LRB), natural rubber bearings (NRB), high-damping rubber bearings (HDRB) and friction pendulum systems (FPS), can help to decrease the maximum response acceleration, base shear and interstory drift (Ali et al., 2024; Bai et al., 2026; Chen et al., 2025; Ghrewati et al., 2023; Rahmia et al., 2025; Solgi et al., 2025). They are dependent on the mechanical properties of the isolating layer. In rubber bearings, these are near-incompressibility, shape-dependent vertical stiffness, lateral flexibility and hysteretic damping. HDRBs absorb energy in the rubber without the need for a lead core or other mechanical components. Therefore, they are easier to produce, less harmful to the environment and more appropriate for local production than lead rubber bearings (Ganji, 2026; Ghrewati & Das, 2021; Jin et al., 2026; Ragni et al., 2025; Wahab & Zhong, 2026). HDRBs are also ideally suited for recycled rubber since the damping is also provided by the rubber component (Gambiro et al., 2023; Ghrewati & Das, 2021). They are easy to make, so can be produced using local resources and simple processing. This is important where the possibility to use advanced seismic protection is restricted due to economic and technological reasons, such as Pakistan, where the seismic risk is high and budget is limited. Concurrently, the automobile industry has generated a significant waste tyre volume, which has led to an accumulation of waste tyres on landfills, as well as to open burning and long-term environmental degradation (Hassan & Rodrigue, 2024). This waste rubber can be used as an engineering material in structural devices within the concept of the circular economy and cleaner production (H.-T. Zhang et al., 2026). The question of whether recycled tyre rubber can provide the stiffness and damping that would be necessary for an isolation layer, is therefore one of material and structural mechanics, which this study examines.

In this study, the mechanical behavior of a locally produced waste tyre rubber base isolator (WTRBI) is studied. The isolator is a laminated rubber part with no lead core or steel shims. Constructed with stacked rubber layers

with basic fabrication methods and utilizing local waste material. The aim is to establish experimentally the potential of the vertical load capacity, lateral flexibility and hysteretic damping of the recycled tyre rubber to be used as an isolation layer, and the effect that the device will have on the response of the structure that it supports. The investigation is at two levels. The reduced size WTRBI was tested for compression and lateral pushover at the device level to determine its vertical stiffness and effective lateral stiffness. The structural level testing included a scaled-down single-storey steel frame, tested with a fixed base and tested on the WTRBI under static pushover, free vibration, impact loading and harmonic excitation loading conditions. Comparing both support conditions, the effect of the isolator on the structure's lateral stiffness, fundamental period, response acceleration, base shear and energy dissipation is shown. The goal is to correlate isolator mechanical characteristics obtained through measurement with the dynamic response of the structure under various loading scenarios. The objective is to relate the measured mechanical characteristics of the isolator with the dynamic response of the structure under different types of loading.

1.1 Global and Local Production of Waste Tyre

The rapid growth of the transportation sector has led to a significant increase in the production and consumption of tyres worldwide, resulting in the accumulation of large quantities of waste tyre rubber (Hassan & Rodrigue, 2024; Hittini et al., 2021; Shahjalal et al., 2021; Yaqoob et al., 2021). Globally, billions of tyres reach the end of their service life each year, creating serious environmental challenges due to their non-biodegradable nature, bulk volume, and potential fire hazards (Dobrotă et al., 2020; Hassan & Rodrigue, 2024; Jalal et al., 2019; Ren & Sancaktar, 2019; Turer & Özden, 2008; Yaqoob et al., 2021). Improper disposal practices, such as open dumping and burning, contribute to soil contamination, air pollution, and public health risks, highlighting the urgent need for sustainable management solutions (Nerea et al., 2026; Turer & Özden, 2008; Wang et al., 2026). In recent years, various approaches have been explored for recycling waste tyres mentioned in table 2, including their use in road construction, energy recovery, roof insulation and rubberized materials as shown in figure 1 (Liu et al., 2026; Nawagamuwa & Bavindi, 2026; Nerea et al., 2026; Özkılıç et al., 2026; Qureshi & Li, 2026; Wang et al., 2026; Wu et al., 2026; Yousafzai et al., 2026; Z. Zhang et al., 2026; Zheng et al., 2026). However, a significant amount of waste tires are still underutilized, especially in poorer nations with inadequate infrastructure and technological improvements for recycling. This offers a chance to recycle used tire rubber into engineering solutions that add value, including seismic isolation devices. At the local level, nations like Pakistan are seeing an ongoing rise in the use of automobiles, which has resulted in a constant increase in the production of waste tires, as seen in table 1. The buildup of abandoned

tires in landfills and public areas due to ineffective recycling methods raises environmental issues (Gorakifard et al., 2026; Jin et al., 2026; Turer & Özden, 2008). Although this material is widely available, its use in cutting-edge technical applications is still mostly unexplored.

Table 1: Annual waste tyre generation (Yaqoob et al., 2021).

Year	Tyre Generation (millions)						
	Cars	Trucks	Buses	Pickups	Farm Tractor	Motorcycles-2W	Rickshaws-3W
2010-2011	$5.5x10^5$	$\sim1x10^4$	$\sim2x10^4$	$1x10^5$	$2.6x10^5$	$1x10^6$	$1.3x10^5$
2011-2012	$6.3x10^5$	$\sim1x10^4$	$\sim2x10^4$	$1x10^5$	$1.5x10^5$	$1x10^6$	$1.5x10^5$
2012-2013	$4.8x10^5$	$\sim1x10^4$	$\sim2x10^4$	$8x10^5$	$2x10^5$	$1x10^6$	$1.1x10^5$
2013-2014	$4.5x10^5$	$\sim1x10^4$	$\sim2x10^4$	$8x10^4$	$1.2x10^5$	$1x10^6$	$1x10^5$
2014-2015	$6.2x10^5$	$\sim1x10^4$	$\sim2x10^4$	$1.5x10^5$	$2x10^5$	$1x10^6$	$1.2x10^5$
2015-2016	$7.3x10^5$	$\sim1x10^4$	$\sim2x10^4$	$1.4x10^5$	$1.4x10^5$	$1x10^6$	$1.4x10^5$
2016-2017	$7.5x10^5$	$\sim1x10^4$	$\sim2x10^4$	$1x10^5$	$1.3x10^5$	$1x10^6$	$1.3x10^5$
2017-2018	$8.5x10^5$	$\sim1x10^4$	$\sim3x10^4$	$2x10^5$	$2.2x10^5$	$3.7x10^6$	$2.4x10^5$
2018-2019	$8x10^5$	$\sim2x10^5$	$\sim3x10^4$	$1.5x10^5$	$2x10^5$	$3.45x10^6$	$2.2x10^5$

The current project turns an environmental burden into a useful structural element by using this locally accessible trash resource to create a high damping base isolator. The research encourages a sustainable and circular strategy, where waste materials are efficiently repurposed to improve structural resilience, by integrating recycled tire rubber into the design of Waste Tyre Rubber Base Isolator (WTRBI). Therefore, incorporating scrap tire rubber into seismic protection systems not only solves the waste management problem but also offers an affordable substitute for traditional materials, which makes it especially appropriate for developing areas with limited financial resources.

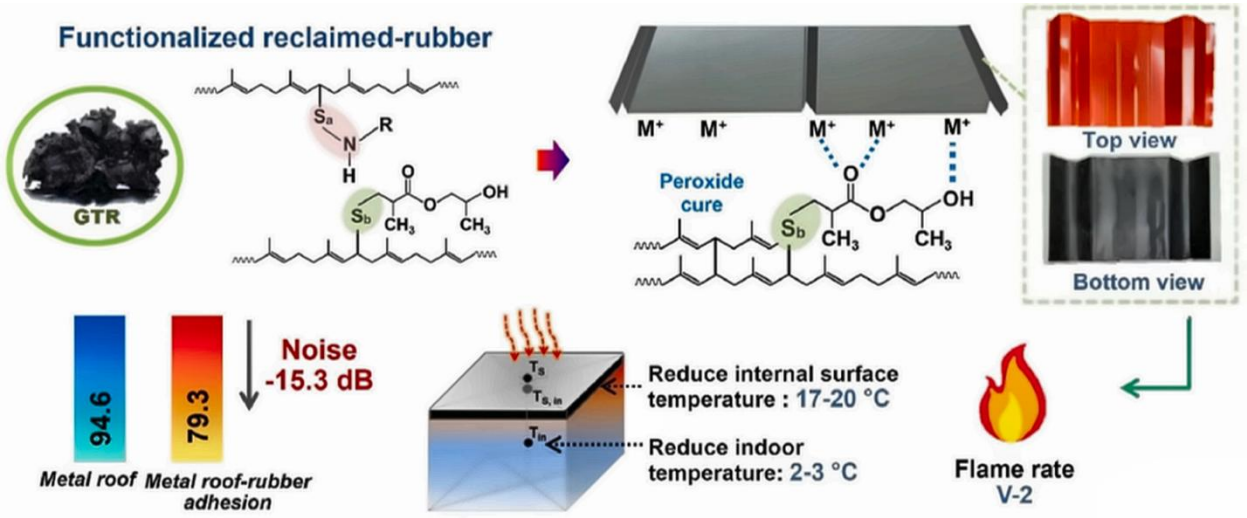

Figure 1: Waste tyre recycling through roof insulating sheets (Siriboon & Magaraphan, 2025).

Table 2: List of available rubbers and their applications (Hassan & Rodrigue, 2024).

Sr. No.	Product Categories	Product Sub-Categories	Applications
Interior Construction Products			
1	Floorings and Mats	Rubber tiles	Residential and commercial buildings, sports, fitness, daycare, agriculture, ice arenas, garages, etc.
		Sports mats	
		Anti-Vibration Mats	
		Warehouse tiles	
2	Flooring underlayment's	Acoustics	Residential and commercial buildings
Exterior Construction Products			
3	Rooftop walkway tiles	-	Industrial or commercial buildings
4	Asphalt paving	-	Residential and commercial outdoors, and parks
6	Landscape tiles	Interlocking tiles and blocks	Residential and commercial outdoors

1.2 Current Practices for Utilization of Waste Tyre

Due to its high-volume accumulation and non-biodegradable nature, waste tire rubber management and usage have become crucial issues. Many techniques for recycling or reusing scrap tires have been developed over time; however, the majority of these techniques concentrate on low-value or energy-intensive applications and have little bearing on high-performance engineering uses. In order to increase flexibility, durability, and resistance to cracking, scrap tire rubber is processed into rubber sheets and powder and added to asphalt mixtures. This is one of the most popular methods used in road building in figure 2. Similar to this, scrap tires are frequently utilized in the manufacture of roofing materials, sports tracks, and playground surfaces because of their advantageous shock-absorbing and sound-insulating qualities (Siriboon & Magaraphan, 2025). Energy recovery is another popular technique, where tires are utilized as fuel in industrial furnaces and cement kilns because of their high calorific value. Furthermore, scrap tires are used in geotechnical engineering applications such drainage layers, embankment stabilization, and lightweight filler material. Although these uses offer some solutions to the disposal issue, they frequently fail to properly utilize rubber's mechanical and viscoelastic qualities, especially its capacity for energy dissipation under dynamic loads. Particularly in poorer nations, advanced applications like the utilization of recycled rubber in vibration isolation pads and seismic protection systems are still very rare and understudied. These applications need performance evaluation and controlled material processing, as seen in figure 2, both of which are frequently absent in local contexts. The current study sets itself apart by using waste tire rubber to create a Waste Tyre Rubber Base Isolator (WTRBI),

transforming the material into a high-performance structural application from traditional low-value usage. By doing this, it illustrates how recycled rubber may be used to effectively dissipate seismic energy, providing advantages for both engineering and the environment. By encouraging a switch from conventional disposal techniques to creative, performance-driven uses, this strategy not only increases the value of waste tire materials but also helps build robust and sustainable infrastructure systems.

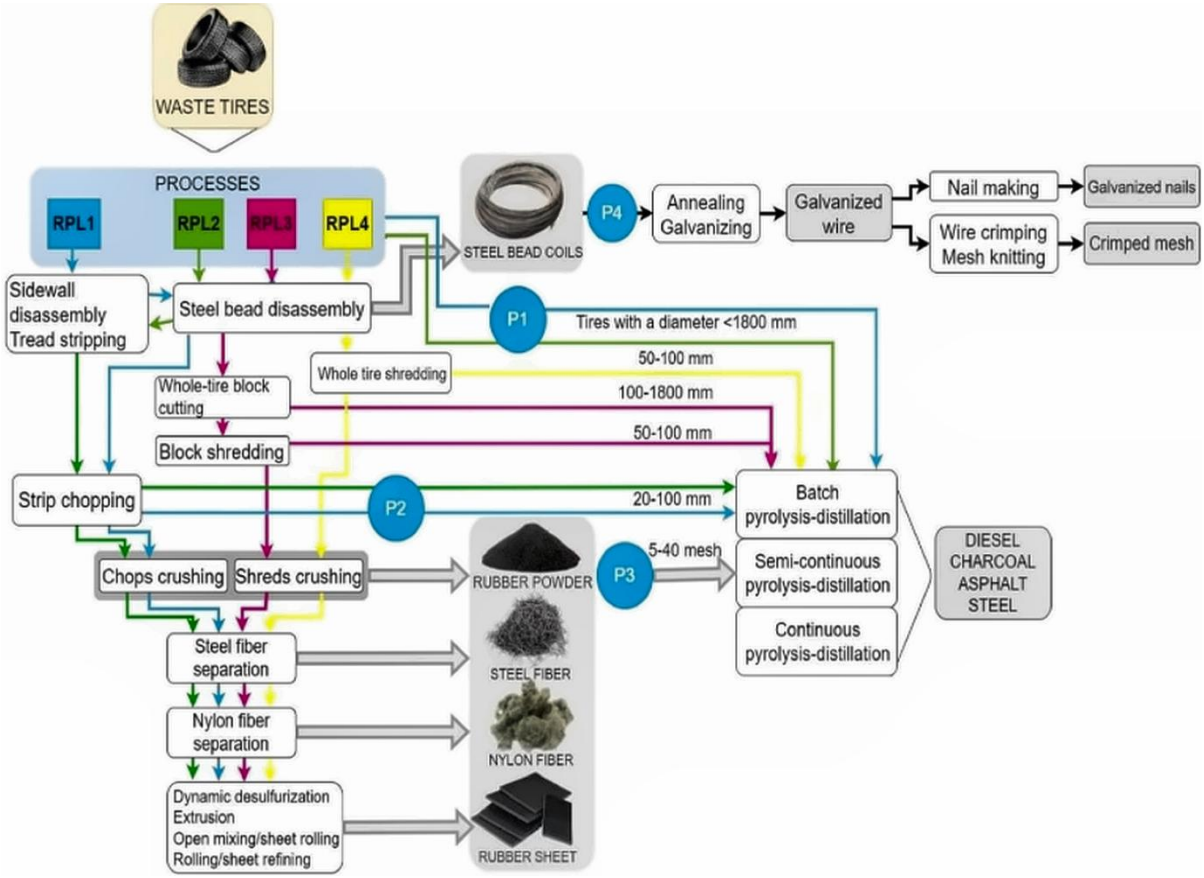

Figure 2: Waste tyre processing (Abdullah, 2024).

1.3 Proposed Technology and Specific Aim of Current Work

In order to improve the seismic resilience of buildings in areas with limited resources, the current study presents an innovative, inexpensive base isolation technique made from recycled waste tire rubber. The suggested system is a locally produced Waste Tyre Rubber Base Isolator (WTRBI), which does away with the need for costly imported equipment and intricate production processes that are frequently connected to traditional isolation systems.

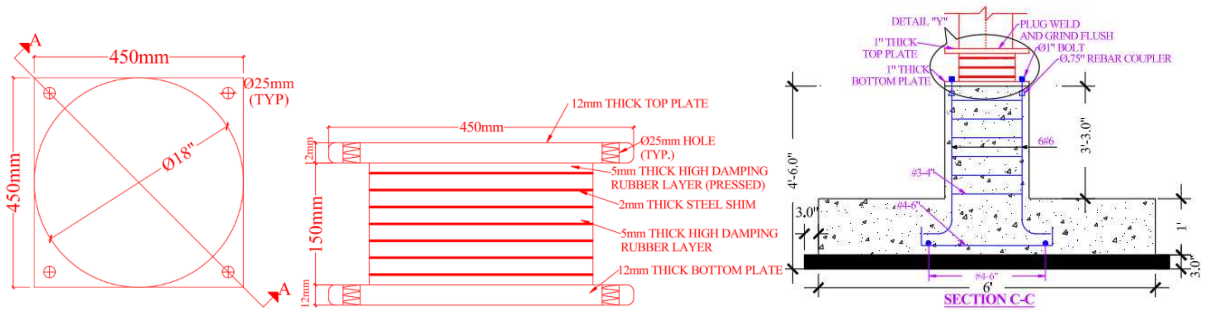

a)

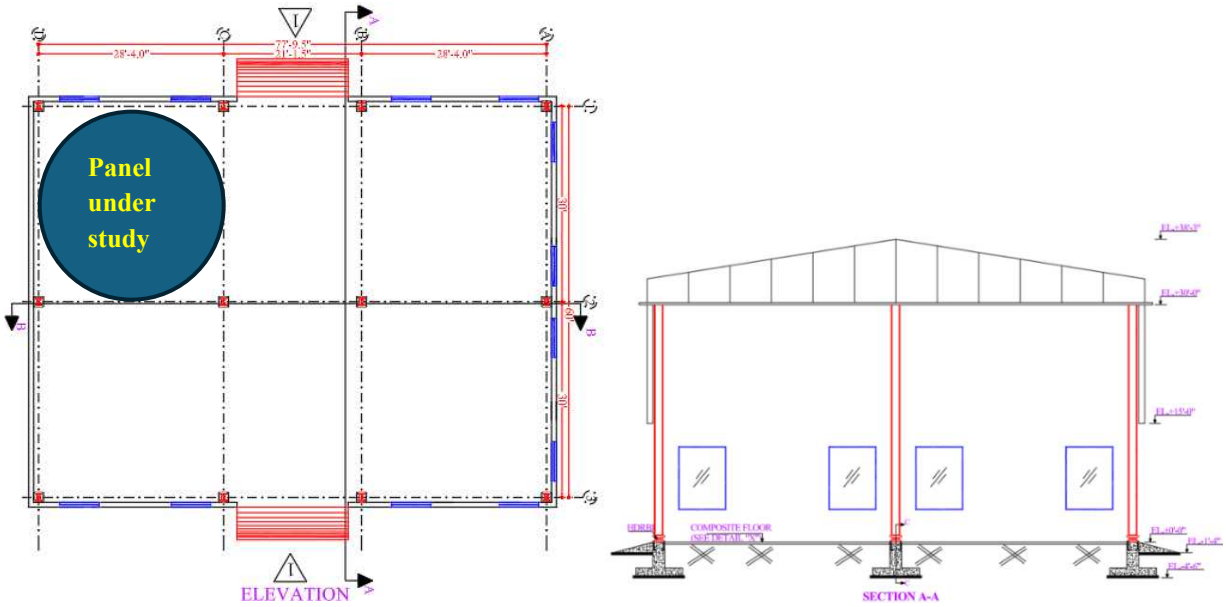

b)

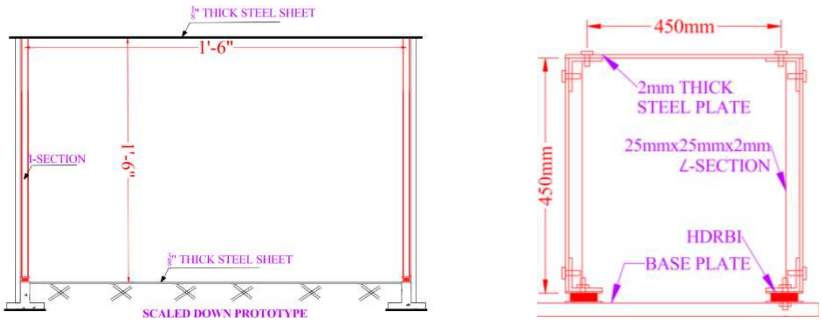

c)

Figure 3: Proposed technology; a) Proposed base isolator (plan & section) and connection with structure; b) Proposed base isolated structure (plan & section); c) Scaled down structure and scaled down structure with simplified boundary conditions.

The suggested technology addresses structural safety, economic viability, and environmental sustainability by making use of locally accessible waste materials. Figure 3 (a), which shows the plan and sectional features of the suggested base isolator along with its connection mechanism with super-structure and sub-structure, illustrates the isolator's conceptual configuration and geometry. The apparatus is made up of multilayer rubber components designed to offer lateral flexibility and a built-in ability to dissipate energy through hysteretic activity. Furthermore, the integration of the isolator within a structural system is depicted in figure 3 (b), showing the plan and sectional views of the proposed base-isolated structure, highlighting the placement and functional role of the isolators at the foundation level. For experimental validation, the proposed structure was scaled down and tested with scaled down WTRBI designed for scaled down prototype structure shown in figure 3 (c). The detailed specifications of the full-scale base isolator for a real building are summarized in table 3.

2. Research Significance

Innovative, affordable, and locally adaptive seismic protection systems are required due to the growing susceptibility of structures to seismic hazards, especially in developing nations (Nerea et al., 2026; Özkılıç et al., 2026; Wang et al., 2026; Yousafzai et al., 2026; Z. Zhang et al., 2026; Zheng et al., 2026; Zhu et al., 2026). The increasing vulnerability of structures to seismic hazards, particularly in developing countries, necessitates the development of innovative, cost-effective, and locally adaptable seismic protection technologies (Apriyono et al., 2026; Darwesh et al., 2026; Jin et al., 2026; Kumar et al., 2026; Moasas et al., 2022). Base isolation has been shown to be one of the most effective methods for reducing the effects of earthquakes, but its widespread use is still restricted in places like Pakistan because of its high initial costs, reliance on imported equipment, and lack of local manufacturing capacity. This study offers a sustainable and financially feasible solution to these problems. The creation of a locally produced Waste Tyre Rubber Base Isolator (WTRBI) from recycled scrap tire rubber, which turns an environmental liability into a useful structural resource, is what makes this work significant. The method minimizes the impact on the environment while simultaneously lowering material costs. The experimental validation of the suggested technique under controlled dynamic settings is another significant addition to this work. This research increases the reliability and application of the findings by using shaking table testing to provide practical proof, in contrast to many studies that only use analytical or numerical methodologies. Clear insights into the system's efficacy in terms of decreased

peak acceleration, base shear, improved energy dissipation, and damping can be obtained by comparing fixed base and base-isolated versions. Additionally, by providing design specifications for full-scale structural application and comprehensive conceptual illustrations of the isolator and its structural integration, as shown in figures 3 (a) and 3 (b), the study closes the gap between laboratory-scale innovation and practical implementation.

Table 3: Specifications of base isolator for proposed real structure.

Properties	Abbreviation	Value
Diameter of WTRBI	D (m)	0.45
Height of WTRBI	H (m)	0.15
Fundamental Period of Structure	T_N (sec)	0.127
Design Period	T_D (sec)	3
Effective Stiffness of WTRBI	$K_{B.eff}$ (N/m)	45.4
Design Displacement	D_D (m)	13
Base Shear on WTRBI	V_B (N)	469.8

3. Development, Testing and Performance of Base Isolator

3.1 Development of Base Isolator

The goal of developing the suggested base isolator was to use recycled waste tire rubber to create an affordable and environmentally friendly Waste Tyre Rubber Base Isolator (WTRBI). In order to obtain the requisite flexibility and energy dissipation properties for seismic isolation, the process included material selection, preparation, geometric configuration, and isolator production. Waste tire rubber was chosen as the main component of the isolator because of its high damping capability, robustness, and accessibility. In order to give lateral flexibility and retain an adequate vertical load-carrying capability, the isolator was developed as a layered rubber system with 22 waste rubber layers. The necessary stiffness and damping qualities were taken into consideration when choosing the geometric configuration, which included diameter, thickness, and number of layers. The suggested technology is still feasible for use in developing countries because the fabrication process was completed utilizing locally accessible methods. To create a single unit that could withstand cyclic loading and display steady hysteretic activity, the layers were put together and bonded. To prevent early failure or inconsistent performance, extra care was taken to ensure consistent bonding and correct alignment.

3.1.1 Preparing Waste Rubber for Base Isolators

One crucial process that directly affects the finished device's mechanical performance, longevity, and energy dissipation capacity is the preparation of waste tire rubber for use in base isolators (Moasas et al., 2022; Turer &

Özden, 2008). As shown in figure 1, a methodical processing process is necessary to transform waste tires into a consistent and dependable engineering material appropriate for seismic applications since they contain impurities including steel wires, textile fibers, and surface pollutants. Waste tires are first collected and separated, and then they are thoroughly cleaned to get rid of dust, grime, and other impurities (Hassan & Rodrigue, 2024; Yaqoob et al., 2021). The tyres are then mechanically processed to separate steel reinforcements and fiber materials, ensuring that only pure rubber content is retained (Abdullah, 2024; Moasas et al., 2022). This stage is crucial to preventing behavioral irregularities and enhancing the final product's bonding qualities (Moasas et al., 2022). Following separation, the rubber is shredded or ground to reduce its size, resulting in either sheet-like or crumb-like rubber, depending on the intended use. After processing, the rubber is further refined and, if needed, reconstituted into layers or pads using binding and compression processes (Moasas et al., 2022). This makes it possible for the material to develop a more uniform structure, which is essential for consistent performance under cyclic loading.

During the layering process, the rubber may be treated with binding agents or adhesives to improve the mechanical qualities, guaranteeing appropriate cohesiveness between layers and preventing delamination during operation (Moasas et al., 2022; Turer & Özden, 2008; Yousafzai et al., 2026; Zaland et al., 2026). The prepared rubber layers are then shaped according to the desired geometric configuration of the base isolator. Special attention is given to achieving uniform thickness, proper alignment, and consistent density, as these parameters significantly affect the stiffness and damping characteristics of the isolator (Gambiro et al., 2023; Ghrewati et al., 2023; Ghrewati & Das, 2021). As a result, the finished rubber material can display consistent hysteretic behavior, which is necessary for efficient dissipation of seismic energy. Waste tire rubber is prepared for use in Waste Tyre Rubber Base Isolator (WTRBI) by turning it from an uneven and polluted substance into a structured, performance-oriented component (Gambiro et al., 2023; Ghrewati & Das, 2021). This step plays a vital role in ensuring that the developed isolator meets the required functional and structural performance criteria.

3.1.2 Development of Base Isolator

The goal of the production of the suggested scaled-down base isolator was to provide a straightforward, affordable, and regionally viable fabrication process for Waste Tyre Rubber Base Isolator (WTRBI) using recycled scrap tire rubber. Table 5 provides the specifics of this technique. Because the process didn't require complex industrial machinery, it could be used in settings with low resources. The rubber material, which is obtained by cleaning used tires, is the first step in the process. The rubber was then shaped into consistent, 1 mm-thick layers that function as the

isolator's main energy-dissipating elements. To reach the necessary height of 25mm, these rubber layers were then stacked. Table 4 compares the scaled-down WTRBI with commercial HDRB. Cyanoacrylate, an adhesive bonding agent, was used between layers during stacking to guarantee correct cohesion and avoid separation during cyclic stress. After that, the assembly is compressed for 12 hours, which enables the layers to properly bind and create a single, cohesive unit.



b)

Figure 4: Manufacturing of scaled down base isolator; a) Geometry of scaled down WTRBI. b) Manufacturing process of WTRBI.

Table 4: Comparison of proposed scaled down WTRBI with commercial HDRB.

Parameter	**Our WTRBI**	**Commercial HDRB**
Rubber Material	Recycled waste tyre rubber	NRB, NBR, ENR, EPDM blends
Manufacturing Cost	PKR 2,000 (scaled down)	PKR 100,000 (full scale)
Adhesive	Cyanoacrylate	Phenolic bonding
Vulcanization	Not vulcanized	Heat-vulcanized
Pressing time	12 hours	1-8 h under heat and pressure

To achieve the required lateral flexibility and vertical load-bearing capability, the geometric dimensions-diameter, thickness, and number of layers-are meticulously regulated. Figure 4 shows the isolator's final configuration with full manufacture, including its plan and sections details. The isolator was constructed with consideration for

uniformity, alignment, and surface quality in order to enhance structural integrity and performance consistency. These elements are necessary to guarantee dependable performance under repeated loading circumstances and stable hysteretic behavior. Because the manufactured WTRBI doesn't require lead cores or steel shims like traditional base isolators do, the production process is much simpler and less expensive. The developed manufacturing approach is scalable for the matching full-scale design specifications given in Table 3, making it practically applicable. This ensures that the proposed technology can be extended from laboratory prototypes to real-world structural applications.

Table 5: Material and geometrical specifications of scaled down base isolator.

Properties	Units	Value
Diameter of Base Isolator	mm	25
Height of Base Isolator	mm	25
Thickness of Rubber Layer	mm	1
Dimension of Top/Bottom Plate	mm	25 x 25
Thickness of Top/Bottom Plate	mm	2
Number of Layers	-	22
Rubber Used	-	Waste tyre rubber

3.2 Test setups for Developed Base Isolator

3.2.1 Compression Test

The purpose of the compression test was to assess the developed Waste Tyre Rubber Base Isolator (WTRBI) stiffness properties and vertical load-carrying capacity. (Chen et al., 2025; Sierra et al., 2019). This test is essential to ensure that the isolator can safely support the gravity loads of the superstructure while maintaining its functional integrity under service conditions. This test is necessary to make sure the isolator can sustain the superstructure's gravity load safely while retaining its functional integrity in service. To provide a consistent distribution of compressive force, the isolator specimen was positioned between two rigid steel plates in a load-controlled compression testing machine, as shown in figure 5 (a). A compression machine was used to gradually apply a vertical load, and the isolator's corresponding deformation reaction was noted. Important test data, including applied load, vertical displacement, and horizontal displacement, were tracked and recorded in table 6.

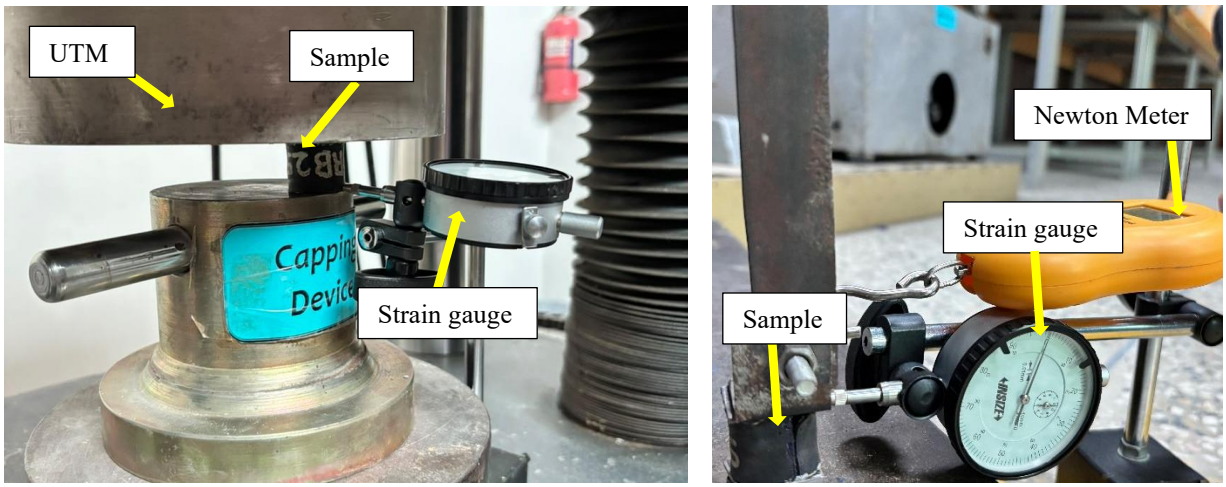

a) b)

Figure 5: Test setup for base isolator; a) Under compression loading. b) Under pushover loading.

The vertical stiffness of the isolator, a crucial factor in base isolation design, was ascertained using the resulting load-deformation relationship. To avoid excessive settlement and enable the isolator to operate efficiently under lateral seismic loads, sufficient vertical stiffness is required. Additionally, the compression behavior sheds light on the waste rubber's material consistency and elastic stability. The isolator can consistently support structural loads without suffering appreciable deterioration or irreversible deformation if it responds steadily and almost linearly within the working load range.

3.2.2 WTRBI Pushover Test

The developed Waste Tyre Rubber Base Isolator (WTRBI) lateral deformation capacity was assessed using the pushover test. This test is essential for evaluating the isolator's performance under repeated seismic loading, which exposes structures to cyclic displacements as opposed to monotonic forces (Chen et al., 2025; Sierra et al., 2019). In order to replicate the real service state of a structure, the isolator specimen was exposed to lateral loading utilizing spring balance while keeping a constant vertical compressive stress of 132.8 N. As seen in figure 5 (b), the specimen was positioned between the structure and base plate, and a spring balance was used to apply lateral displacement in a controlled manner. Throughout the test, the associated force and displacement responses were continually recorded. Repeated cycles of rising displacement amplitudes, which represented various seismic demand levels, made up the loading process. This made it possible to assess how the isolator behaved in both minor and high deformation ranges.

Plotting the resultant force-displacement curves allowed for an analysis of the device's stiffness properties. The effective lateral stiffness of the isolator can be directly determined from the curve's form and slope.

3.3 Performance of Base Isolator

3.3.1 Compression Behavior

To determine whether the created Waste Tyre Rubber Base Isolator (WTRBI) could safely support vertical loads while preserving structural stability and functional integrity, its compression behavior was examined. (Chen et al., 2025; Sierra et al., 2019; Turer & Özden, 2008). Because the isolator must sustain the dead and live loads of the superstructure without suffering from excessive deformation or material deterioration, this characteristic is crucial in base isolation systems. The isolator demonstrated a steady and constant load-deformation response under progressively increasing compressive loads, as depicted in figure 6, according to the compression test results detailed in Section 3.2.1. The isolator has the necessary elastic stiffness for structural applications since the relationship between applied load and vertical displacement was almost linear throughout the operating range. The developed base isolator supported a maximum load of 3.16 kN with permanent vertical strain of 0.913 and lateral strain of 0.244, according to the observed compression response. This indicates that waste tire rubber can provide adequate vertical load-bearing capacity when assembled and prepared correctly. After that, Poisson's ratio was computed, and the result was 0.48, indicating that it can safely support the vertical loads while sustaining higher lateral stresses. Since a perfectly incompressible material should have a Poisson's ratio of 0.5, the measured value of 0.48 shows that the waste tire rubber is almost incompressible. This demonstrates how the rubber layers expand laterally when compressed vertically while keeping a nearly constant volume. Since it enables the isolator to carry the vertical structural stresses with good efficiency while staying highly flexible in the horizontal direction, the near incompressibility trait is an intrinsic feature of elastomers and a prerequisite for effective base isolation. The success of the material preparation and manufacturing process is demonstrated by the lack of notable indications of instability, buckling, or premature failure with preload of 132.8N.

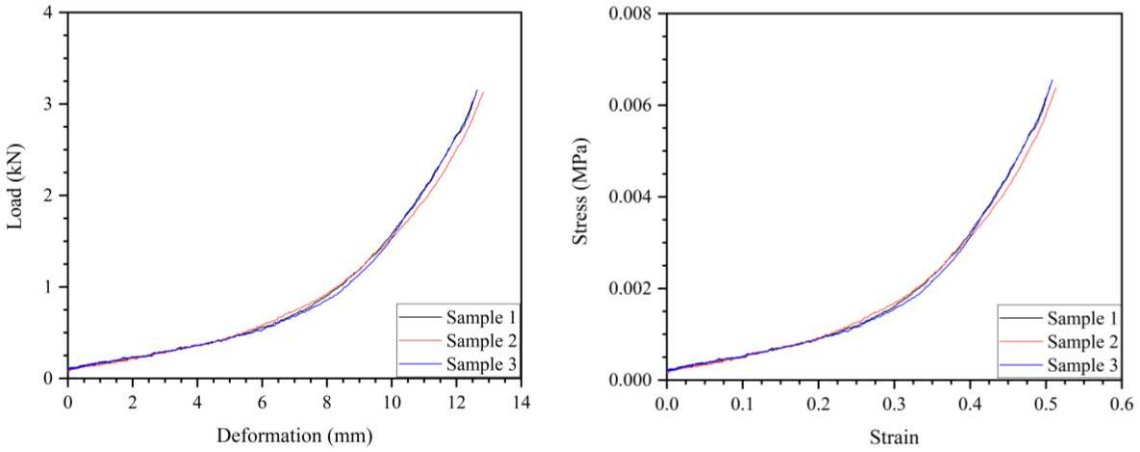

a) b)

Figure 6: Results from compression test; a) Load-Deformation Curve. b) Stress-Strain Curve.

Furthermore, as seen by the vertical stiffness of 0.391 kN/mm, the isolator demonstrated controlled deformation characteristics, guaranteeing that vertical displacements stay within allowable bounds under service loads. This is necessary to keep the structure aligned and effective, as well as to avoid unwanted settlements (Turer & Özden, 2008). A monolithic response underload is the result of good rubber layer bonding, which is indicated by the lack of irregularities or abrupt stiffness changes. Overall, the findings show that the proposed WTRBI is acceptable for supporting structural loads while permitting the required lateral flexibility for seismic isolation since it achieves the basic criteria of sufficient vertical stiffness paired with stability.

Table 6: Mechanical properties of base isolator.

Test	Strength (kN)	Stiffness, K_{Ver} (kN/mm)	Compression Modulus (kN/mm^2)	Vertical Strain, ε_{ver}	Lateral Strain, ε_{lat}	Poisson's Ratio, v
Compression	3.167±0.04 (1.28)	0.391±0.043 (11.05)	0.0123±0.00027 (2.16)	0.509±0.003 (0.63)	0.244±0.013 (5.26)	0.48±0.022 (4.61)

[1] Standard Deviation (±).
[2] Coefficient of Variance (CV %).

3.3.2 Stiffness Behavior

One important measure of the developed Waste Tyre Rubber Base Isolator (WTRBI) efficiency in seismic energy dissipation and lateral flexibility is its stiffness behavior. Because structures experience multiple displacement reversals under earthquake stress, the isolator must demonstrate a stable and consistent hysteretic response under cyclic deformation (Talaeitaba et al., 2019). Figure 7 illustrates the isolator's well-defined and stable curve under loading cycle based on the pushover testing previously discussed. The curve shows the material's capacity for effective

energy absorption and dissipation, which is essential for lowering the seismic forces transferred to the superstructure. The isolator's response did not significantly deteriorate in strength or stiffness over the course of subsequent cycles. Furthermore, the isolator demonstrated adequate lateral deformation capability, enabling it to withstand seismic displacements without failing.

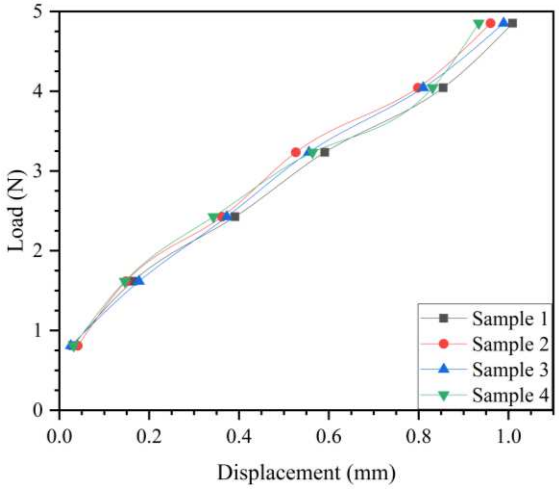

Figure 7: F-Δ curve for WTRBI.

When compared to the stiffness of the structure, the effective lateral stiffness determined during testing was 0.891N/mm, which is ideal for base isolation systems. It guarantees harmony between solidity and adaptability. Overall, stiffness behavior confirms that the designed base isolator operates effectively under dynamic loading circumstances, making it a dependable and useful seismic isolation option. Table 7's findings support the use of recycled scrap tire rubber in real-world structures by showing that it can successfully mimic the hysteretic properties needed for high-performance isolation systems.

Table 7: Results of WTRBI pushover test.

Test	Preload (N)	Stiffness, K_B (N/mm)	Max Strain, ε
Pushover	132.8	0.891±0.059 (6.61)	0.039±0.002 (3.87)

[1] Standard Deviation (±).
[2] Coefficient of Variance (CV %).

3.4 Comparison with Previous Studies

Table 8 compares the results of earlier seismic isolation experiments with the performance of the suggested Waste Tyre Rubber Base Isolator (WTRBI), which was created utilizing recycled scrap tire rubber. The majority of

conventional HDRBs documented in the literature are produced with expensive natural rubber compositions. Increasing damping and lateral flexibility dramatically lowers structural acceleration and vibration response during earthquakes, according to earlier research on elastomeric and rubber-based isolators (Abe et al., 2004; Bhaskar & Khanchandani, 2018; Crowder & Becker, 2017; Dall'Asta & Ragni, 2006). Similar behavior was observed in present research. The isolator exhibited stable behavior and effective stiffness characteristics comparable to those reported for conventional HDRBs. Furthermore, the obtained horizontal stiffness and deformation capacity were found to fall within acceptable ranges reported in earlier studies on elastomeric seismic isolation systems (Robinson & Tucker, 1981; Weisman & Warn, 2012). Although the stiffness properties lightly differ from industrially manufactured isolators, the developed system provides a practical and economical alternative for low-rise and small-scale structures, particularly in developing countries where cost-effective seismic protection solutions are required.

Table 8: Comparison with other proposed base isolators.

Proposed by	Diameter (mm)	Thickness of Rubber Layer (mm)	Total Number of Rubber Layer	Thickness of Steel Shim	Lateral Stiffness (N/mm)	Max Displacement (mm)
Basshofi et al. 2019	350	7	15	0.5	490	90mm at 50kN
Robinson and Tucker	600	-	-	5	1700	45mm at 160kN
Kalpakidis and Constantinou	1000	6.7	30	4.8	-	400mm at 1200 kN
Weisman and Warn	152	3	20	3	-	70mm at 18kN
Our WTRBI	25	1	22	-	0.8905	1.009mm at 4.85N

4. Validation of Developed Base Isolator Through Structural Testing

4.1 Development of Prototype Structure

The base isolated real structure was proposed as shown in figure 3 (b) with dimensions of 23337.5mm x 18000mm center-center with a clear roof height of 9000mm. One panel of 8500mmx 9000mm was taken for study. The specific objective of this experimental study was to compare fixed base structure and base isolated structure under dynamic loading. Prototype testing provides specifications for a real or proposed structure, as opposed to a theoretical one. The prototype structure and construction method used in this investigation are based on the methods presented in the literature (Ali, 2018). The goal of this research was to investigate the base isolated structure's dynamic behavior. The structural period is one of the most important factors that depend on the height of the structure (UBC-97).

Table 9: Properties of elements used for prototype structure.

Element	Material	Property	Dimension (mm)
Column	Steel	L-Section	25 x 25 x 2
Slab	Steel	Raised-Pattern Floor Plate	450 x 475 x 2
Connection	Steel	Bolted	Ø 6.3
Bolt	Steel	A449 Structural Fasteners	Ø 6
Base Plate	Steel	Guage 18 Floor Plate	650 x 675 x 3.125

The scale-down technique is mainly applied in the elevation dimensions of the structural height measurements. There are three components of earthquake forces i.e. x, y and z components. It would be simpler to understand behavior in one direction. In the present work, the behavior with different magnitudes in one direction is studied. The structure height is an important aspect determining the structural time-period. Thus, the entire scale structure is scaled down using 1/20 scale for elevation dimensions only and thicknesses were not scaled. Table 9 provides details of the prototype. The proposed scaled down WTRBI has a plan dimension of 450 mm x 450mm x150 mm and 4 bolts in the top plate and bottom plate. Total thickness of proposed WTRBI is 174 mm including the 12mm thick top and bottom steel plates as shown in figure 3 (a). Similarly, for prototype construction, the dimensions used in the study are 25mm x 25mm x 25mm with a total thickness of 29 mm including the 2mm thick top and bottom plates as shown in figure 4 (a). The prototype used in this study consists of a scaled down steel structure designed to represent the dynamic characteristics of a steel building when equipped with a locally made WTRBI as shown in figure 8 (b).

The model was constructed using steel sections due to the uniform characteristics of steel, ease of fabrication, and consistency in mechanical behavior. The prototype structure comprises a single-story, single-bay frame, having plan dimensions of 450mm x 475mm center to center and clear height of 450mm, framed with L-shaped steel angles of 25mm × 25mm × 2mm, connected through bolts to maintain geometric accuracy while allowing slight flexibility representative of real structures. The floor masses were simulated by attaching 2mm thick steel plate, providing a distributed mass of approximately 4.3 kg on floor, resulting in a total structural mass of 6 kg. The column base was connected with locally made WTRBI which was mounted on base plate as shown in figure 8 (c). The WTRBI consists of alternating layers of waste rubber each 1mm thick layer, providing effective lateral stiffness appropriate for scaled down dynamic testing. Steel shims were not used in the WTRBI as their primary role is to enhance the load carrying capacity and in this scaled modeling the rubber layers are providing enough vertical stiffness to carry incoming loads.

This prototype setup allows for realistic simulation of vibration modes, energy dissipation behavior, and isolation performance under dynamic loading.



a) b)

Figure 8: Real prototype structures for testing; a) Scaled down fixed base prototype with simplified boundary conditions; b) Scaled down base isolated prototype with simplified boundary conditions.

4.2 Instrumentation and Parameters to be Explored

Two distinct base conditions were used to evaluate the prototype structures: (i) all four columns were fixed, and (ii) four columns had a locally manufactured Waste Tyre Rubber Base Isolator. Measuring the frame's lateral stiffness changes when it is supported by WTRBI as opposed to being fastened directly to the base plate was the main objective of the pushover testing. As seen in figure 9 (a), the lateral static load was manually applied at the roof level of the frame. A load cell was used to measure the applied lateral force, and a scale was used to record the corresponding displacement of the roof. The load gradually increased up to a target load of 196 N. Three pushover tests were performed for each support condition (fixed-base and WTRBI-isolated) in order to confirm the repeatability of the results. Dynamic properties of the structure, such as fundamental frequency (fn) and damping ratio (ξ), play an important role in determining the overall dynamic behavior of a structure (Ali et al., 2013). To assess the dynamic properties of both structural configurations, i.e., (i) fixed base condition and (ii) structure with locally made WTRBI, snap-back tests were conducted. Figure 9 (b) illustrates the experimental setup used for the snap-back test. A wire of 300 mm length was attached at the top of each structure to apply lateral displacement. The structures were displaced by 6 mm and 12mm at the roof level using the attached wire and subsequently released suddenly to induce free vibration. This displacement level was selected to ensure elastic behavior of the structure and isolator while providing

sufficient response amplitude for reliable identification of dynamic parameters. Free vibrations of the structures were observed immediately after releasing the wire, allowing the inherent dynamic characteristics to be captured without external excitation. To record the structural response, an ADXL345 three axis accelerometer with 13-bit resolution was mounted at the top of both structures, while an additional accelerometer was installed on the base plate to verify the authenticity and consistency of the measured response. During the recording process, minor noise was observed in the acceleration time-history data due to vibrations and sensor sensitivity. Initially, a MATLAB filtering technique was employed to remove excessive noise, followed by further signal refinement using SeismoSignal software through a bandwidth filtering. Finally, the acceleration time histories were obtained, and the logarithmic decrement method was used to calculate the damping ratio (ξ) and fundamental frequency (fn) of the scaled-down steel structure with different support conditions.

The maximum force and acceleration imparted to the structure, the maximum deflection of the structure, and the fundamental frequency and damping ratio of each structural design are the dynamic parameters of primary relevance in an impact loading scenario (Cao et al., 2026; Chen et al., 2026; Li et al., 2026). Both the fixed-base (FBP) and base-isolated (BIP) prototype configurations underwent controlled impact tests to assess these. As depicted in figure 9 (c), impact loading was imparted by hammering each prototype's column base. In order to simulate a brief impulsive stimulation, the impact was delivered as a single, controlled blow that was aimed horizontally at the column base. Twelve impact tests were conducted, six on the FBP and six on the BIP, utilizing a hammer strike to ensure input comparability. The entire system reaction was recorded using three ADXL345 three-axis accelerometers with 13-bit resolution: To capture the acceleration reaction from the point of impact application, Accelerometer 1 (ACC-1) was installed at the base of the impacted column and to measure the amount of acceleration response produced at the top of the construction, Accelerometer 2 (ACC-2) was fixed to the roof level. The hammer was equipped with Accelerometer 3 (ACC-3). Using Newton's second law (F = m*a), the force applied by the hammer blow was calculated using the acceleration time history and the hammer's known mass (0.89 kg). These three-accelerometer setups allow for the simultaneous measurement of the impact's acceleration and force on the column. Small levels of noise from vibrations and vibrations from the surrounding environment due to sensor sensitivity were included in the acceleration data gathered from the time history records. As previously mentioned, filtering was used to eliminate these disruptions. For harmonic loadings, a basic uniaxial shake table constructed locally was used. There was no

additional bulk on top of the structure due to the shake table's payload limitations. Finding the maximal energy dissipation resulting from the use of locally built WTRBIs was the main objective of this testing.

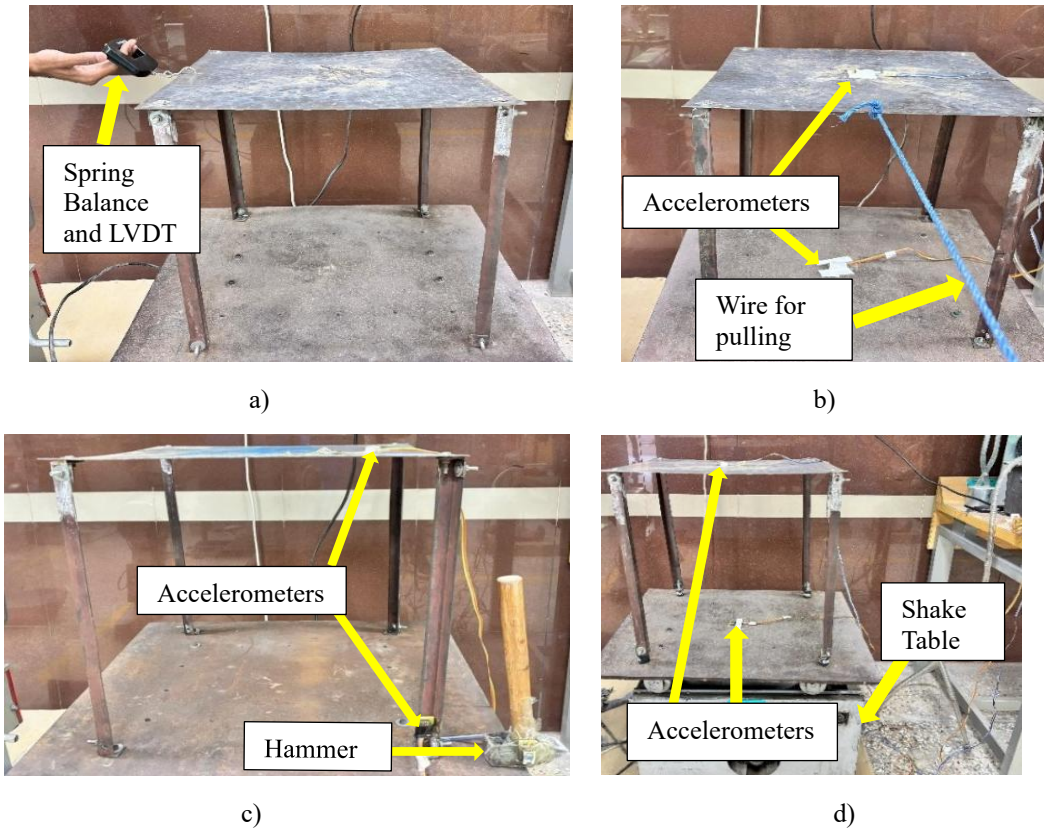

Figure 9: Instrumentation; a) For pushover test. b) For snap-back test. c) For impact loading. d) For harmonic loading.

Two accelerometers were employed in this configuration to measure structural reaction, as seen in figure 9 (d). The structure was instrumented using the following set of accelerometers: one on the roof to record the response acceleration on top of the diaphragm and another at a shake table to record the applied acceleration. The natural frequency was used to determine the number of excitation frequencies. These frequencies were chosen in accordance with the base isolated prototype structure's fundamental natural frequency, which was determined to be 3.2 Hz. When a structure is excited at a frequency close to its natural frequency, phenomena of resonance may occur, resulting in maximum displacement ultimately resulting maximum structural damage. Accordingly, frequencies of 2.8Hz, 3.6Hz are less than and greater than the natural frequency of 3.2 Hz were applied to investigate the dynamic response of the structure under resonance conditions. Acceleration time histories were used to access the prototype structure's response with WTRBI during each test. Additionally, acceleration data was used to create hysteresis curves. The base shear (Q)

was computed using the formula $Q = M\ddot{U}$, where M is the prototype structure's mass (6 kg) and $\ddot{U}_R$ is the measured acceleration (response acceleration) at the top of the structure. Lastly, the base-isolated steel prototype's energy dissipation and corresponding damping ratios were assessed.

4.3 Performance of Model Structure

4.3.1 Structural Stiffness

The primary goal of the pushover tests is to measure the amount that the frame's lateral stiffness when it is supported by WTRBI rather than fixed directly to the base plate. The lateral static load was manually applied at the frame's roof level using a spring balance. The measured force-displacement data was used to determine the frame's global lateral stiffness in each configuration. Using the straightforward formula k=F/Δ, the stiffness for a given displacement level Δ is calculated using the corresponding lateral force F from the load cell. A set of stiffness values were obtained for both the fixed-base and WTRBI-supported configurations by repeating this calculation at successive displacement steps as reported in table 10. The force displacement curve's shown in figure 10 have small-displacement region, where the response is linear. This makes it possible to compare the two support conditions directly and shows how the WTRBI affects the frame's overall lateral stiffness.

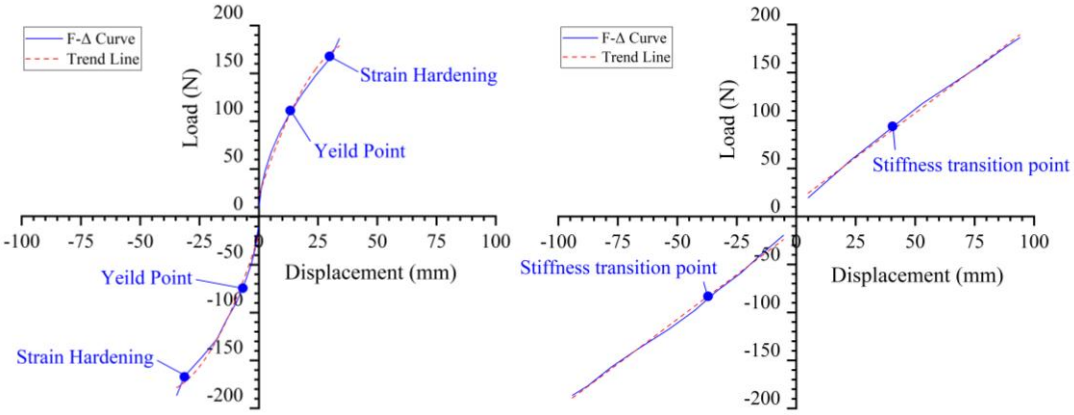

Figure 10: Load-Deformation Curve; a) For fixed base prototype structure. b) For base isolated prototype structure.

The pushover tests made force-displacement (F-Δ) curves that show how the frame's lateral resistance changes when the roof is displaced for both fixed-base (FBP) and WTRBI-isolated setups. These curves show how

stiff the system is. There were six tests in total: three on the fixed-base frame and three on the WTRBI-supported frame. Every test had a maximum load of 186.39N. The F-Δ curves for the fixed-base frame shown are representative of all the test results. The trend across the displacement range is steep and almost linear. The WTRBI-supported frame has a slope that is more gradual, which means it is less stiff and can bend more to the side when the load is the same. The fixed-base F-Δ curve shows sharp initial stiffness and a clear yielding plate around 12-15 mm of displacement, which is typical of steel frame behavior. WTRBI-isolated curves show that the material gets softer over time and has a much flatter slope from the start. The consistent 63.8% stiffness reduction 5.482N/mm and 1.983N/mm at 186.39N for fixed base and base isolated prototype structures across multiple tests shows that local WTRBI works well for seismic isolation.

Table 10: Structural stiffness.

Prototype	**Max Load, P (N)**	**Max Displacement, Δ (mm)**	**Static Stiffness, $K_{S,\ FBP}$ (N/mm)**
Fixed Base	186.39	34	5.482
Base Isolated	186.39	94	1.983

4.3.2 Natural Frequency (fn) and Damping Ratio (ξ)

The Ü-t curves from the snapback tests give a depiction of the free-vibration response of the both fixed-base (FBP) and base-isolated steel prototype structures (BIP) right after sudden release of imposed lateral displacement as illustrated in figure 11. These curves give a direct graphical representation of the dynamic behavior of the system that tracks the oscillatory behavior, amplitude decay as well as the vibration period of the structure. In total 12 tests were performed, six on the FBP with an amplitude of 6mm and six with an amplitude of 12mm. The oscillations in figure 11 show the damping performance of the steel structure with the locally made Waste Tyre Rubber Base Isolator (WTRBI) compared to the oscillations of fixed base structure. The basic time-period of the structures was calculated by time intervals between successive peaks in the Ü-t curves and logarithmic decrement method was used to compute the damping ratio, despite gradual reduction in acceleration of response, which shows the energy dissipation ability of the base isolated structure which are reported in table 11. An oscillation amplitude that decays more quickly implies the presence of damping, which is caused by the WTRBI, and a increase in natural period indicates the decrease of effective stiffness, which is caused by base isolation. The comparison of the curves drawn in the fixed base support condition and the base isolated support condition indicated an increment in natural time-period of the base isolated structure. The base isolated system exhibits more steady and natural oscillatory behavior than the sharp response of

the fixed base system. The likelihood of structural damage under the effect of inertial force in the seismic excitation is minimized.

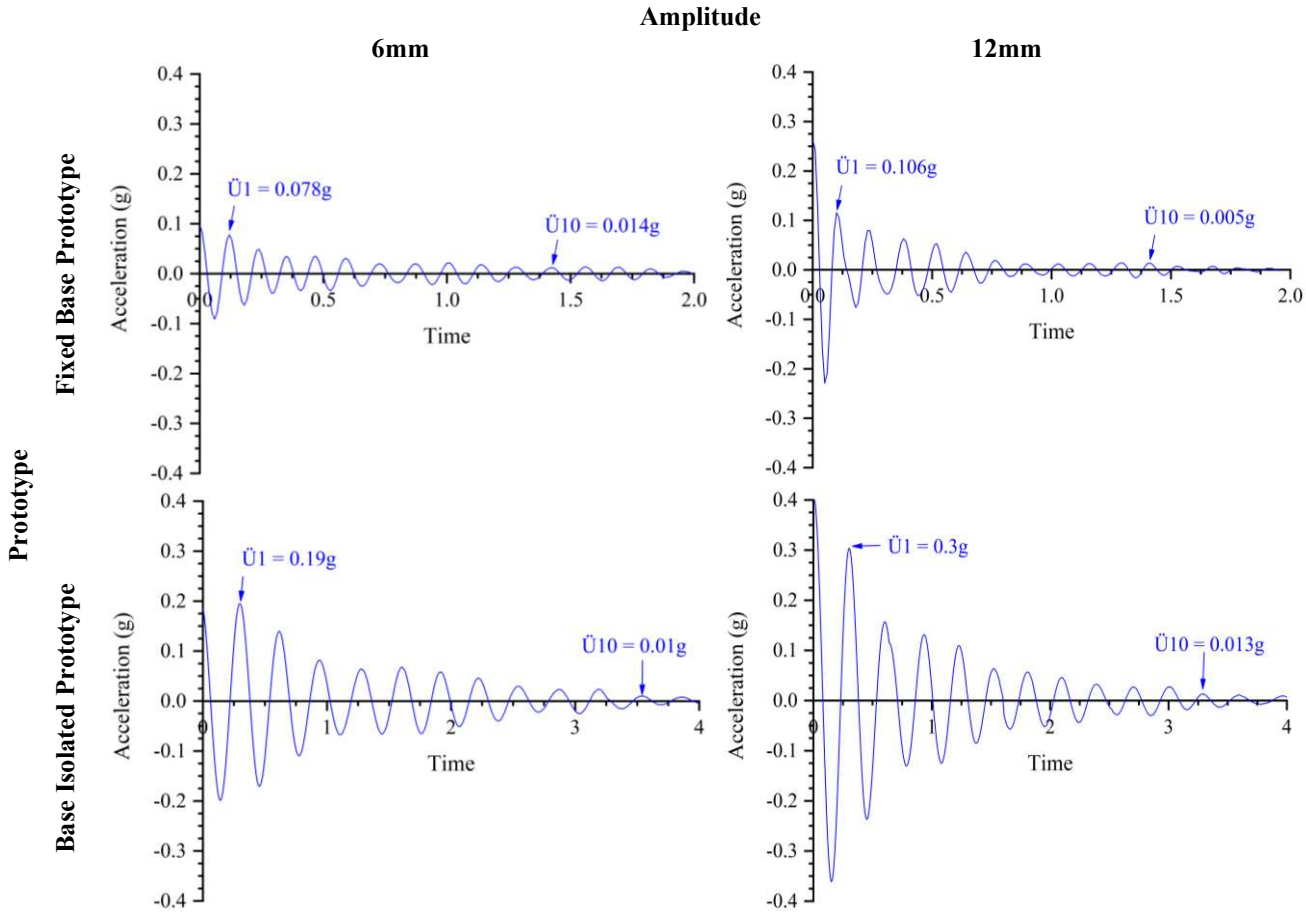

Figure 11: Ü-t Curves from snap-back test.

The experimentally obtained dynamic properties of the prototype structural models with fixed base (FBP) and high damping rubber base isolator (BIP) are summarized in table 9. The damping ratio (ξ) of the prototype structures with different supports were calculated by the log decrement method using the acceleration time history curves shown in figure 11. For the structure with a fixed base (FBP), the fundamental time-period (T_n) was determined as 0.13 sec, corresponding to a fundamental frequency (f_n) of 7.6 Hz. The calculated damping ratio (ξ) was 3.3%. In contrast, the structure equipped with high damping rubber base isolators exhibited a significantly increased fundamental time period of 0.31 sec and a reduced fundamental frequency of 3.2 Hz. The damping ratio of the base isolated structure increased to 5%. The increase in time period and decrease in fundamental frequency of the BIP

verify the effect of shifting the period of structures due to base isolation. Moreover, an increase in damping ratio of the BIP verifies the effect of damping increased by Waste Tyre Rubber Base Isolator (WTRBI).

Table 11: Dynamic properties of prototype structures (fn and ξ).

Structure	Dynamic Properties			
	Amplitude (mm)	**Tn (s)**	***f*n (Hz)**	**ξ (%)**
Fixed base prototype (FBP)	6	0.13±0.01 (4.6)	7.6±0.08 (0.99)	3±0.26 (8.02)
	12	0.13±0.01 (4.5)	7.6±0.07 (0.95)	3.3±0.06 (1.68)
Base isolated prototype (BIP)	6	0.32±0.01 (3.7)	3.1±0.1 (2.4)	5±0.06 (1.2)
	12	0.30±0.01 (3.8)	3.3±0.1 (2.6)	4.9±0.1 (4.7)

[1] Standard Deviation (±).
[2] Coefficient of Variance (CV %).

The values given in parentheses represent the Coefficient of Variance (CV), which shows the percentage of dispersion of the experimental results. The calculated CV values of frequency for fixed base prototype structure against 6mm and 12mm amplitudes are 0.99 and 0.95 respectively, while those for the damping ratio are 8.02 and 1.68. These values are in acceptable range (<10%), indicating minor variability in the experimental measurements. A CV of 8.02 for damping ratio suggests little higher scatter in the calculated damping ratio values, implying that the results may be influenced by experimental uncertainties such as accelerometer sensitivity or inconsistencies in snapback release. Moreover, this is not uncommon in damping estimation because damping is highly sensitive to peak selection, signal noise, and logarithmic decrement calculations. Experimental damping values for the fixed base prototype structure typically show more scatter compared to natural frequency. Overall, the low CV values for the dynamic properties (fn, Tn and ξ) are in acceptable range. To improve the accuracy of the test results, it would be beneficial to increase the number of trials, improve signal filtering, or refine peak-selection methods to reduce variability.

4.3.3 Performance Under Impact Loading

The acceleration time-history (Ü-t) curves obtained from the impact tests on the fixed-base prototype (FBP) and the base-isolated prototype (BIP) are shown in figure 12. The free vibration response of the structure after the hammer blows at the bottom of the column is shown by each curve. In tandem, the following records from ACC-1 (column base), ACC-2 (roof level) and ACC-3 (hammer) give full information on impact force input, column response and transmitted superstructure response.

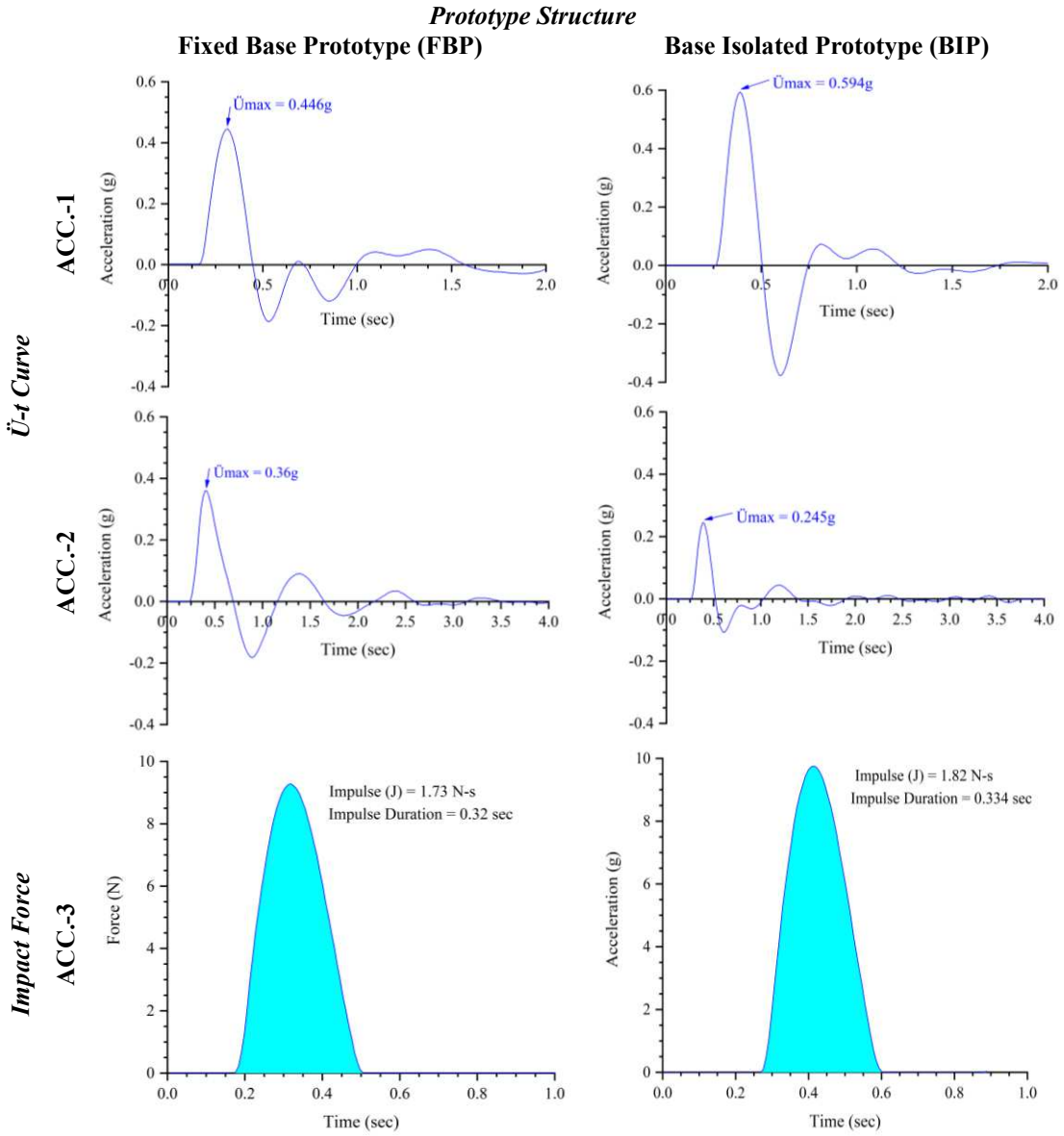

Figure 12: Results from impact loading.

The prototype with a fixed base shows the closely coupled amplitudes of the Ü-t curves corresponding to ACC-1 and ACC-2, with the roof level response (ACC-2) being very close to the one recorded at the column base (ACC-1). The near unity value here indicates that there is little restriction on the transmission of energy through the structural system due to the fixed connection. The damping of the fixed-base steel frame is low, and the oscillations dampen relatively slowly. By contrast, the base-isolated prototype exhibits strong decoupling of the column base response (ACC-1) from the roof response (ACC 2). The column base acceleration is reduced by WTRBI to 0.25g at the roof, which is good confirmation that the impact energy is intercepted and dissipated by the WTRBI before it can

travel to the superstructure. The post-impact free vibrations of the BIP also decay faster, which is also an indicator of the effects of the rubber isolator's hysteretic energy dissipation and internal material friction. In addition, the oscillation period of the Ü-t curve of the BIP is longer than that of the FBP. This period elongation is a result of the reduction of effective stiffness caused by the WTRBI, which is an important part of the base isolation system that is effective at high frequencies that are associated with an impulsive input.

The quantitative dynamic properties obtained from the impact tests of both structural configurations are given in table 12. The results show that the locally manufactured WTRBI is effective in changing the structural response under impact loading. The peak base column acceleration ($Ü_B$) and peak roof response acceleration ($Ü_R$) for the prototype with fixed base are very close, which means full force transmission through the rigid base connection. For the FBP fundamental frequency was 0.95 Hz and damping ratio was 18.1%. The base isolated prototype has a significantly different response. The WTRBI reduced the peak roof response acceleration by about 32.43% as compared to the acceleration at the base of the column, showing the effectiveness of the WTRBI in isolating the superstructure from the impact induced forces. The natural frequency went down from 0.95 Hz to 0.54 Hz, which is 43.16% less, and it is the natural time-period which was increased. The damping ratio was raised from 18% to 21%, which verified the increased energy dissipation ability of the structural system by the WTRBI. The results are also consistent with those of the dynamic properties measured from a similar prototype under snapback and harmonic loading conditions, thereby demonstrating consistency of the performance of the isolator for different loading types.

Table 12: Results of impact tests conducted on each prototype configuration.

Dynamic Properties	**Fixed Base Prototype**	**Base Isolated Prototype**	**% Change**
Imparted Force, F (N)	9.3	9.7	+4.3
Max. force at Roof Level, F_R (N)	18.14	12.26	-32.41
Column Base Acceleration, $Ü_B$ (g)	0.45	0.6	+33.33
Roof Acceleration, $Ü_R$ (g)	0.37	0.25	-32.43
Fundamental Frequency, fn (Hz)	0.95	0.54	-43.16
Damping Ratio, ξ (%)	18.1	21.1	+16.57

4.3.4 Energy Redistribution and Equivalent Damping (Ęe)

Figure 13 shows the results of the Base-Isolated Prototype (BIP) and the Fixed-Base Prototype (FBP) when subjected to harmonic excitation. This loading was performed with a unidirectional shake table with an input amplitude

of ±25 mm that was constant. The curves that are used in quantifying the Peak Ground Acceleration ($\ddot{U}_G$) in respect to the resulting Peak Response Acceleration ($\ddot{U}_R$) provide a good graphical comparison of the way the two structures behaved during the continuous harmonic excitation. These harmonic loading cycles reveal the ability of the system to reduce or enhance ground motion in real-time as compared to free-vibration experiments. Table 13 shows FBP and BIP responses corresponding to harmonic loadings at frequency 2.8Hz, 3.2 Hz and 3.6 Hz. The FBP Ü-t curves show that the peak response acceleration ($\ddot{U}_R$) immediately follows the acceleration of the ground and shows an average reduction in $\ddot{U}_R$ of 25.7%. This indicates that ground forces are being transmitted to the maximum on fixed support. On the other hand, the BIP Ü-t curves indicate a reduction in the response. When the WTRBI managed to uncouple the superstructure with the motion of the ground, a much less rocky and smaller amplitude oscillation is generated. The basic dynamic characteristics such as base shear, redistribution of energy and equivalent damping that illustrate the enhanced capability of the base isolated structure in connection to the ground forces were calculated using the Ü-t curves are shown in table 13. Based on the comparison of harmonic response curves, it can be said that the natural time period of the base-isolated condition is considerably longer. The base-isolated system was more consistent and natural in its oscillation behavior, whilst the fixed-base system responds promptly and tracked the higher-frequency in the ground motions inputs. The base shear was significantly reduced because the WTRBI alters the basic period of the structure of the frequency of the harmonic excitements. Such a shift is in comparison to the shake table and ensures the superstructure works through a lower spectral acceleration. The hysteretic behavior of the WTRBI was evidenced by the fact that the exponent of the peak response acceleration ($\ddot{U}_R$) decreases continuously. The forces of inertia applied to the structural elements are reduced greatly by the check that the maximum acceleration is reduced by more than 48% relative to the response on a fixed base as indicated in table 12. This reduction in inertial force reduces the potential of structural fatigue or failure under extended dynamic loads. The findings are consistent with proof that the WTRBI developed locally is effective in improving dynamic performance. Also, the noted variation of the response proves the fact that the isolator was effective at eliminating the harmonic energy, so the forces of the ground motion would not reach the upper structure.

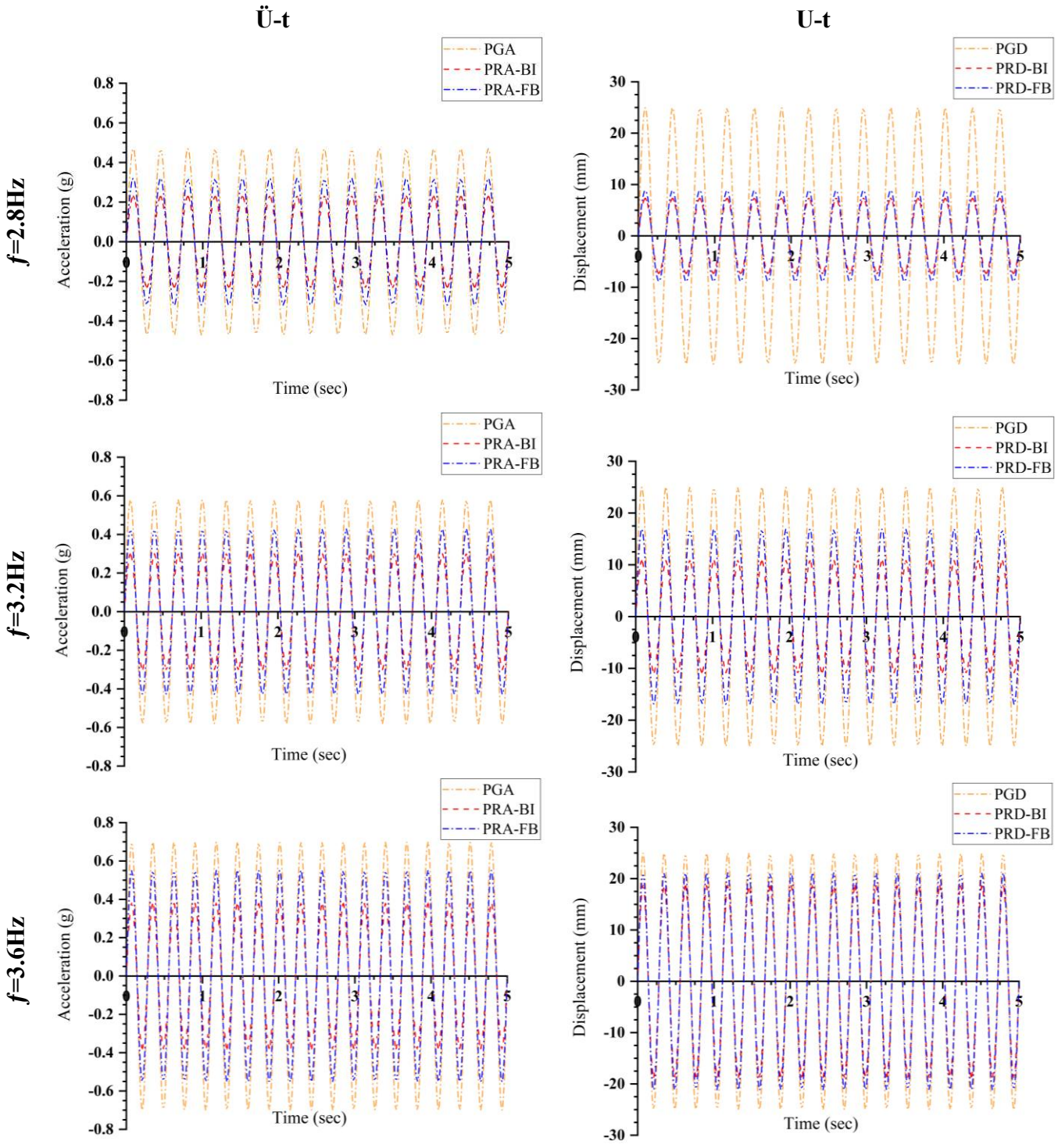

Figure 13: Results from harmonic loading.

The Q-Δ curves were developed to evaluate the structure energy redistribution ability, stiffness degradation and non-linear response data of the structure subjected to harmonic loading. In these graphs, Δ equals the corresponding lateral movement taken by integrating acceleration-time histories from the SeismoSignal software, and Q equals the lateral base shear (computed as the product of response acceleration and structural mass). The experimental data indicates that the fixed-base experiment leads to a Q-Δ curve that has a thin, linear shape which does not have any significant contained area or hollow loop as depicted in figure 14. On the fixed base prototype, the base shear is at peak values of approximately 32.9 N which is a high-stiffness system that can be considered to lack significant viscous damping of ~5.6%. The base-isolated frame equipped with the Waste Tyre Rubber Base Isolator (WTRBI) bears much larger and more prominent hysteresis loops. Figure 14 base isolated structure loops result in obvious hollow loops in which the flexibility of the system is depicted in a great way and energy is lost through hysteresis. The base isolated structure base shear was reduced, and it emerged at approximately 22.9 N even with lateral movement of 18.75 mm worth of energy much less than that of fixed base which demonstrates that the WTRBI was effective in reducing the transmission of ground motion to the super structure with an equivalent viscous damping of ~14%. Damping effect of the rubber isolator was quantitatively expressed with the augmenting of the area of an enclosed loop caused by structural hysteresis and internal friction means of materials. The equivalent viscous damping ratio (ξe) was obtained by the area within each loop.

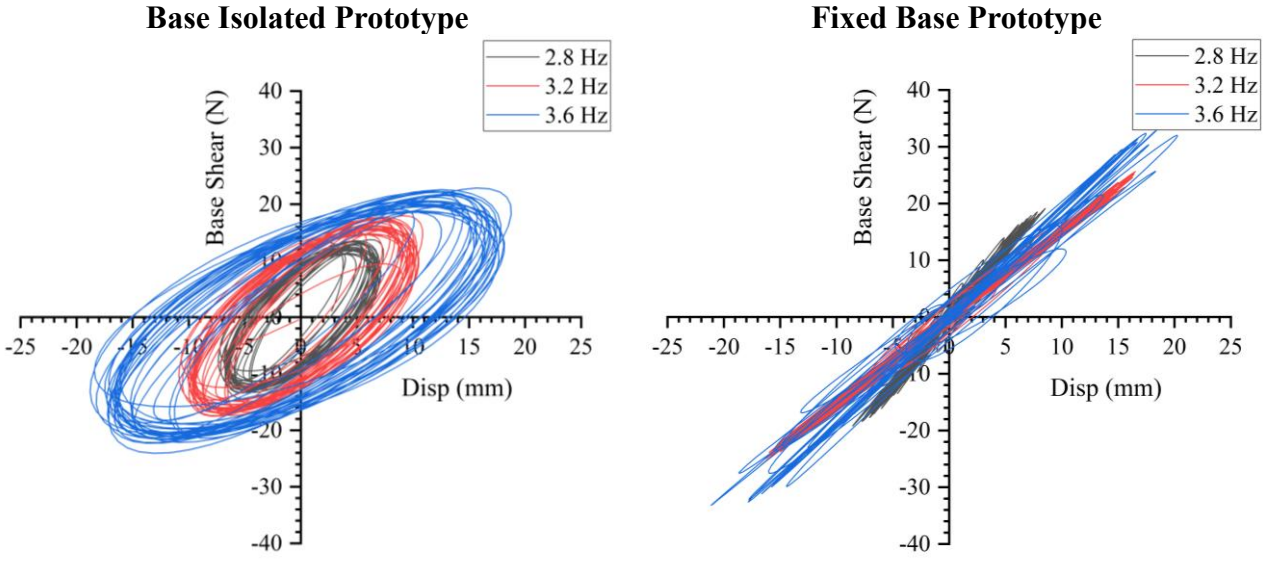

Figure 14: Q-Δ Curves.

Table 13: Energy absorption performance under harmonic excitation.

	Properties	Fixed Base Prototype	Base Isolated Prototype	% Variation
***f*n=2.8 (Hz)**	Peak Ground Acceleration, $\ddot{U}_G$ (g)	0.47	0.47	±0
	Peak Response Acceleration, $\ddot{U}_R$ (g)	0.32	0.23	-28.13
	Peak Ground Displacement, U_G (mm)	25	25	±0
	Peak Response Displacement, U_R (mm)	8.56	7.35	-14.14
	Base Shear, Q (N)	19.1	13.73	-28.12
	Redistributed Energy, $E_{\xi R}$ (N.mm/cyc)	515.3	317.1	-38.46
	Equivalent Damping, ξ_e (%)	4.6	13.8	+200
***f*n=3.2 (Hz)**	Peak Ground Acceleration, $\ddot{U}_G$ (g)	0.58	0.58	±0
	Peak Response Acceleration, $\ddot{U}_R$ (g)	0.43	0.3	-30.23
	Peak Ground Displacement, U_G (mm)	25	25	±0
	Peak Response Displacement, U_R (mm)	16.93	10.85	-35.91
	Base Shear, Q (N)	25.6	18	-29.69
	Redistributed Energy, $E_{\xi R}$ (N.mm/cyc)	1348	612	-54.60
	Equivalent Damping, ξ_e (%)	7	13	+85.71
***f*n=3.6 (Hz)**	Peak Ground Acceleration, $\ddot{U}_G$ (g)	0.7	0.7	±0
	Peak Response Acceleration, $\ddot{U}_R$ (g)	0.55	0.38	-30.91
	Peak Ground Displacement, U_G (mm)	25	25	±0
	Peak Response Displacement, U_R (mm)	21.14	18.75	-11.31
	Base Shear, Q (N)	32.9	22.9	-30.40
	Redistributed Energy, $E_{\xi R}$ (N.mm/cyc)	2188	1345	-38.53
	Equivalent Damping, ξ_e (%)	5.2	15.1	+190.38

5. Role of this Research Outcome in Real Life Application

The findings from this work show the viability of using waste tyre rubber to develop sustainable earthquake protection technology for earthquake resilient infrastructure. With cleaner production, the developed Waste Tyre Rubber Base Isolator (WTRBI) provides a new solution to recycle the discarded tyre waste into a high value structural safety device (Clemente et al., 2019; Sienkiewicz et al., 2017; Turer & Özden, 2008). The suggested method is an affordable, locally produced substitute for the traditional imported seismic isolation systems and a step toward minimizing environmental contamination brought on by the buildup of waste tires. The experimental findings confirmed that the suggested WTRBI may improve structural damping performance and efficiently decrease the transmission of seismic forces. The practical use of seismic protection systems will be significantly impacted by research's findings, especially in developing nations where the adoption of cutting-edge technical solutions is sometimes hampered by financial and technological limitations. By combining affordability, ease of use, and dependable performance, the suggested Waste Tyre Rubber Base Isolator (WTRBI), which was created using recycled

waste tire rubber, offers a competitive alternative to traditional base isolation systems. The proof that locally accessible waste materials can be converted into useful structural elements capable of lowering seismic demand is one of the work's most significant accomplishments. The designed isolator can greatly improve the seismic performance of structures, as demonstrated by the experimental results, which include decreases in peak acceleration and base shear as well as improved energy dissipation and damping. This makes it ideal for residential buildings, low-to mid-rise structures, and vital institutions like hospitals and schools in earthquake-prone areas (Ghrewati & Das, 2021; Sierra et al., 2019). The inclusion of full-scale design specifications guarantees that the suggested technology can be immediately applied in real-world settings rather than being restricted to laboratory-scale validation. These specs can be used by engineers and practitioners to create and install base isolation systems that are suited to regional building methods. Furthermore, a thorough understanding of the installation and integration of the isolator into structural systems is made easier by the conceptual representations shown in figures 3(a) and 3(b).

Economically speaking, the developed WTRBI greatly lessens reliance on imported isolation devices, which lowers project costs and increases accessibility to seismic protection. Local enterprises can make these devices using simple fabrication techniques thanks to the streamlined production process, which eliminates the need for lead cores and intricate mechanical components. This encourages technology transfer and the development of local capacity (Gambiro et al., 2023; Ghrewati & Das, 2021). Additionally, by addressing the problem of waste tire disposal, this research advances sustainable development. The study promotes a circular economy strategy, which reuses waste materials in high-value engineering solutions rather than discarding or burning them, by integrating recycled rubber into structural applications (Meng et al., 2026; Nawagamuwa & Bavindi, 2026; Özkılıç et al., 2026; Qureshi & Li, 2026; Yousafzai et al., 2026; Zaland et al., 2026). Furthermore, confidence in the dependability and durability of the suggested system is increased by successful experimental validation using compression and dynamic response evaluation. This offers a solid basis for future advancements, such as standardization, mass manufacturing, and incorporation into building rules and design specifications. In conclusion, the research offers a scalable, sustainable, and financially viable method for seismic risk mitigation, bridging the gap between invention and practical implementation. It shows that locally developed technology may effectively defend against earthquakes, opening the door for safer and more robust infrastructure in areas with limited resources.

6. Conclusion

By creating a locally produced Waste Tyre Rubber Base Isolator (WTRBI), the study emphasizes the value of utilizing recycled scrap tire rubber as a sustainable building resource for seismic protection applications. The developed base isolator was experimentally evaluated by compression and pushover tests for its vertical load carrying capacity and lateral stiffness behavior. In addition, a scaled-down single-story steel prototype structure was built and tested under fixed-base and base-isolated conditions. The dynamic performance evaluation was conducted by snap-back, pushover, harmonic loading and impact loading tests. From the experimental results following conclusions are drawn:

- The developed WTRBI was able to utilize recycled waste tyre rubber for the necessary stiffness, load carrying capacity and energy dissipation performance for seismic isolation applications which are increasing at rate of 0.40 million tyres per year.
- The results of the compression test confirm that the developed WTRBI can safely support vertical structural loads with linear load-deformation behavior, achieving a maximum load capacity of 3.16 kN with max Δ_{ver}=12.5mm and $\boldsymbol{\varepsilon}_{ver}$=0.509.
- WTRBI showed near-incompressible behavior from Poisson's ratio=0.48 and sufficient K_{ver}=0.391 show the effective bonding between layers and verify its capability to support structure while maintaining the seismic isolation performance.
- The results of the pushover on WTRBI indicate that the WTRBI exhibited little stiffness degradation under lateral loading. The value of effective lateral stiffness=0.891 N/mm indicates its flexibility and confirms its suitability for efficient seismic isolation applications.
- The pushover tests results show that the stiffness of the WTRBI system was reduced in a stable way about 63.8%, which confirms the effectiveness of the system to improve the lateral flexibility.
- The snapback test results demonstrate that the WTRBI modified the dynamic response by increasing the natural time period from 0.13 sec to 0.31 sec, demonstrating enhancement in damping of +40% from 3% to 5%.
- The impact test results demonstrate that the WTRBI improved impact resistance and lowered roof response to -32%, decreased natural frequency to -43%, and enhanced +16% damping ratio.

- From the results of harmonic loading, on average for all the three excitation frequencies the WTRBI lowered response acceleration to ~30%, base shear to ~29.6%, and increased equivalent damping to ~158.7% as compared to the fixed-base system.
- The study shows that waste tyre rubber can be converted into an affordable and environmentally friendly Waste Tyre Rubber Base Isolator (WTRBI) that can greatly lower seismic forces and improve structural damping.

Waste tyres can be utilized to make structure saving devices and, in this study, WTRBI developed from waste tyre rubber showed a reduction in response acceleration by ~30%, base shear by ~29.6% and increased equivalent damping by ~158.7% confirming waste tyre rubber as an affordable and effective seismic isolation solution.

Acknowledgement

The author would like to thank every person who helped throughout the research work, particularly Engr. Dr. Sheryar Ahmad, Engr. Waseem Akram, Mr. Nadeem, Mr. Raheel Mehmood and Mr. Naveed.

References

1. Hassan, M.R. and D. Rodrigue, *Application of Waste Tire in Construction: A Road towards Sustainability and Circular Economy.* Sustainability, 2024. **16**(9): p. 3852.
2. Zhang, H.-T., et al., *Development of a gravity-driven self-centering rubber bearing for seismic isolation.* Soil Dynamics and Earthquake Engineering, 2026. **208**: p. 110392.
3. Zelleke, D.H. and V.A. Matsagar, *Experimental Investigation on Energy-Based Semi-Active Response Control Strategy for Base-Isolated Structures.* Earthquake Engineering & Structural Dynamics, 2026. **55**(1): p. 232–249.
4. Yang, H., et al., *Three-dimensional decoupling isolation bearing: Experimental validation, design methodology, and seismic response.* Soil Dynamics and Earthquake Engineering, 2026. **200**: p. 109920.
5. Razavian Amrei, S.A., et al., *Effect of Ductility Level on the Seismic Behavior of Low Reinforced Concrete Moment-Resisting Frames Equipped by Double Friction Pendulum Bearings Isolation.* Journal of Rehabilitation in Civil Engineering, 2026. **14**(1).
6. Ragni, L., F. Micozzi, and A. Dall'Asta, *Simulation of push and release tests on HDRBs-based isolation systems accounting for viscous effects.* Procedia Structural Integrity, 2026. **78**: p. 2094–2101.
7. Zhang, J., et al., *A Novel FPB-based Isolation Method at Tower–Nacelle Interface for Seismic Performance Enhancement of Onshore Wind Turbines.* International Journal of Structural Stability and Dynamics, 2026: p. 2750192.
8. Xiang, Y., et al., *Damage-Free Wind-Restraint Device for a Base-Isolated Building Structure: Configuration and Prototype Test.* Journal of Structural Engineering, 2026. **152**(1): p. 04025234.
9. Wahab, A.G. and T. Zhong, *Seismic performance and energy dissipation of hillside reinforced concrete buildings isolated by high-damping rubber bearings: a DHI model-based study.* Innovative Infrastructure Solutions, 2026. **11**(2): p. 53.
10. Pratama, A.Y. and I. Ariani, *The Application of Base Isolation System as Earthquake Resisting Technology on Mulya Medika Hospital, Samarinda.* Applied Mechanics and Materials, 2026. **931**: p. 61–71.
11. Gallardo, J.A., et al., *Earthquake Response Sensitivity of HDRB Base-Isolated Hospitals to the Crustal San Ramón Fault in Santiago, Chile.* Earthquake Engineering & Structural Dynamics, 2026.

12. Solgi, M., et al. *Seismic resilience evaluation of a 3D steel moment frame building with triple friction pendulum isolators*. in *Structures*. 2025. Elsevier.
13. Bai, J., et al., *Vibration Isolation Performance of an Inerter–Stiffness–Damping Isolator Mounted on a Flexible Base and Feedback Control.* International Journal of Structural Stability and Dynamics, 2026. **26**(01): p. 2550257.
14. Rahmia, Y., S.A. Osmana, and M.Y.M. Yatima, *Performance Analysis of Structure with Variation in the Cross-sectional Shapes of RC Columns Using Base Isolation.* Jurnal Kejuruteraan, 2025. **37**(3): p. 1419–1426.
15. Chen, P., et al., *Enhancing seismic resilience in base-isolated structures: A performance-based comparison of HDRB and LRB isolation systems.* Engineering Structures, 2025. **342**: p. 120945.
16. Ali, A., et al. *Experimental investigation of sliding-based isolation system with re-centering functions for seismic protection of masonry structures*. in *Structures*. 2024. Elsevier.
17. Ghrewati, B.E., et al., *Effect of replacing the lead core with rubber on the mechanical properties of lead rubber bearing.* Materials Today: Proceedings, 2023. **74**: p. 627–635.
18. Jin, H., et al., *Upcycling Waste Rubber Powders into Reprocessable Reclaimed Rubber with Excellent Damping Properties: Enabled by Dynamic Bonds and Chemical Foaming.* ACS Sustainable Chemistry & Engineering, 2026. **14**(9): p. 4434–4446.
19. Ganji, A.H., *Numerical study on the optimal effective damping ratio of lead-rubber bearings in RC shear-wall structures under far-and near-fault earthquakes.* Innovative Infrastructure Solutions, 2026. **11**(2): p. 108.
20. Ragni, L., F. Micozzi, and A. Dall'Asta, *Long-term viscous effects of in-field tests on HDRBs-based seismic isolation systems.* Engineering Structures, 2025. **339**: p. 120647.
21. Ghrewati, B.E. and M.R. Das, *Study on the Mechanisms of Manufacturing High-Damping Seismic Isolator—HDRB*, in *Current Advances in Mechanical Engineering: Select Proceedings of ICRAMERD 2020*. 2021, Springer. p. 909–918.
22. Gambiro, G., et al., *Design And Production Of Lead Rubber Bearings For Earthquake Absorbers.* Engineering Heritage Journal (GWK), 2023. **4**(1): p. 26–37.
23. Yaqoob, H., et al., *Current Status and Potential of Tire Pyrolysis Oil Production as an Alternative Fuel in Developing Countries.* Sustainability, 2021. **13**(6): p. 3214.
24. Shahjalal, M., et al., *Flexural response of fiber reinforced concrete beams with waste tires rubber and recycled aggregate.* Journal of Cleaner Production, 2021. **278**: p. 123842.
25. Hittini, W., A.-H.I. Mourad, and B. Abu-Jdayil, *Utilization of devulcanized waste rubber tire in development of heat insulation composite.* Journal of Cleaner Production, 2021. **280**: p. 124492.
26. Dobrotă, D., G. Dobrotă, and T. Dobrescu, *Improvement of waste tyre recycling technology based on a new tyre markings.* Journal of Cleaner Production, 2020. **260**: p. 121141.
27. Ren, X. and E. Sancaktar, *Use of fly ash as eco-friendly filler in synthetic rubber for tire applications.* Journal of cleaner production, 2019. **206**: p. 374–382.
28. Jalal, M., N. Nassir, and H. Jalal, *Waste tire rubber and pozzolans in concrete: A trade-off between cleaner production and mechanical properties in a greener concrete.* Journal of Cleaner production, 2019. **238**: p. 117882.
29. Turer, A. and B. Özden, *Seismic base isolation using low-cost Scrap Tire Pads (STP).* Materials and Structures, 2008. **41**(5): p. 891–908.
30. Wang, S., et al., *Outstanding self-healing ability of weathered asphalts endowed with deeply degraded tire rubber.* Journal of Cleaner Production, 2026. **538**: p. 147335.
31. Nerea, B., et al., *Engineering Properties and Applications of Tire-derived Aggregates: A Review.* Transportation Infrastructure Geotechnology, 2026. **13**(4): p. 87.
32. Zheng, F., et al., *Particle effect and interaction effect of scrap tire crumb rubber on adhesion of asphalt-aggregate interface.* Journal of Cleaner Production, 2026. **554**: p. 147959.
33. Zhang, Z., et al., *Circular valorization of waste tires using spent fluid catalytic cracking (sFCC) catalyst: sustainable aromatic upgrading and sulfur immobilization.* Journal of Cleaner Production, 2026. **557**: p. 148258.
34. Yousafzai, A.K., et al., *An Experimental Study on the Influence of Waste Tyre Metal Fibre on Asphalt Mixture's Performance Properties.* Materials, 2026. **19**(5): p. 849.
35. Wu, M., et al., *Asphalt-rubber interaction in crumb rubber modified asphalt: A review.* Journal of Cleaner Production, 2026. **546**: p. 147766.
36. Qureshi, M. and J. Li, *Structural behaviour of reinforced rubberised concrete beam with waste tyre steel fibres.* Engineering Structures, 2026. **353**: p. 122230.

37. Özkılıç, Y.O., et al., *Thermo-mechanical and data-driven assessment of sustainable concrete incorporating waste tire aggregates and recycled steel fibers.* Buildings, 2026. **16**(5): p. 946.
38. Nawagamuwa, U.P. and C.D.S. Bavindi, *Advancing Circular Economy: Utilizing Shredded Scrap Tyres in Gabion Wall Construction.* Advances in Science and Technology, 2026. **177**: p. 93–100.
39. Liu, C., et al., *Effects of recycled rubber crumbs on the maintenance behavior of a new composite ballast bed.* Journal of Cleaner Production, 2026. **550**: p. 147912.
40. Gorakifard, M., J.E. Sierra, and E. Kian Far, *Polymer extrusion processes in tire manufacturing: a systematic review and bibliometric analysis.* The International Journal of Advanced Manufacturing Technology, 2026: p. 1–48.
41. Siriboon, J. and R. Magaraphan, *Devulcanization and functionalization of ground tire rubber for the novel metal sheet roof with strong sound absorber and thermal insulation.* Cleaner Engineering and Technology, 2025. **24**: p. 100865.
42. Abdullah, Z.T., *Expansion of a mechano-chemical plant for remanufacturing waste tires into rubber sheet and profitable wire steel by-products: A quantitative sustainability assessment.* Applications in Engineering Science, 2024. **17**: p. 100164.
43. Zhu, Z., C. Tai, and Y. Lu, *Modified waste tire rubber for heavy metal immobilization and performance enhancement of cement-based materials.* Journal of Building Engineering, 2026. **119**: p. 115371.
44. Kumar, R., M. Sadique, and M.M. Alam, *Enhancing rockfall barrier performance using waste used car tyres: A step towards sustainable civil engineering.* Journal of Cleaner Production, 2026. **538**: p. 147353.
45. Darwesh, H., et al., *Sustainability Evaluation of Using Waste Rubber in Treating Soft Clay Subgrades for Road Embankments.* The Egyptian International Journal of Engineering Sciences and Technology, 2026. **53**(1): p. 26–34.
46. Apriyono, A., et al., *Stability of Slopes Reinforced with a Combined Waste Tyre and Vetiver System.* Geotechnical and Geological Engineering, 2026. **44**(2): p. 125.
47. Moasas, A.M., et al., *A worldwide development in the accumulation of waste tires and its utilization in concrete as a sustainable construction material: A review.* Case Studies in Construction Materials, 2022. **17**: p. e01677.
48. Zaland, S., et al., *Surface treatments of waste tyres for sustainable concrete production: A performance, environmental and cost-based review.* Construction and Building Materials, 2026. **521**: p. 146141.
49. Sierra, I.E.M., et al., *Development and experimental behavior of HDR seismic isolators for low-rise residential buildings.* Engineering Structures, 2019. **183**: p. 894–906.
50. Talaeitaba, S.B., M.M. Pourmasoud, and M. Jabbari, *An innovative base isolator with steel rings and a rubber core.* Asian Journal of Civil Engineering, 2019. **20**(3): p. 313–325.
51. Dezfuli, F.H. and M.S. Alam, *Shape memory alloy wire-based smart natural rubber bearing.* Smart Materials and Structures, 2013. **22**(4): p. 045013.
52. Islam, A.S., et al., *Non-linear time domain analysis of base isolated multi-storey building under site specific bi-directional seismic loading.* Automation in construction, 2012. **22**: p. 554–566.
53. Ishii, K., et al., *Coupling behavior of shear deformation and end rotation of elastomeric seismic isolation bearings.* Earthquake engineering & structural dynamics, 2017. **46**(4): p. 677–694.
54. Abe, M., J. Yoshida, and Y. Fujino, *Multiaxial behaviors of laminated rubber bearings and their modeling. I: Experimental study.* Journal of Structural Engineering, 2004. **130**(8): p. 1119–1132.
55. Dall'Asta, A. and L. Ragni, *Experimental tests and analytical model of high damping rubber dissipating devices.* Engineering Structures, 2006. **28**(13): p. 1874–1884.
56. Crowder, A.P. and T.C. Becker, *Experimental investigation of elastomeric isolation bearings with flexible supporting columns.* Journal of Structural Engineering, 2017. **143**(7): p. 04017057.
57. Bhaskar, G. and M. Khanchandani, *A Review On Seismic Response Of Building With Base Isolation.* International Journal Of Scientific Research And Review, 2018. **7**(1): p. 92–96.
58. Weisman, J. and G.P. Warn, *Stability of elastomeric and lead-rubber seismic isolation bearings.* Journal of Structural Engineering, 2012. **138**(2): p. 215–223.
59. Robinson, W. and A. Tucker, *Test results for lead-rubber bearings for WM. Clayton building, Toe Toe bridge and Waiotukupuna bridge.* Bulletin of the New Zealand Society for Earthquake Engineering, 1981. **14**(1): p. 21–33.
60. Ali, M., *Role of post-tensioned coconut-fibre ropes in mortar-free interlocking concrete construction during seismic loadings.* KSCE Journal of Civil Engineering, 2018. **22**(4): p. 1336–1343.
61. Ali, M., R. Briet, and N. Chouw, *Dynamic response of mortar-free interlocking structures.* Construction and Building Materials, 2013. **42**: p. 168–189.

62. Li, L., et al., *Understanding the dynamic compressive behaviors and damage evolution of low-carbon ultra-high performance concrete under impact loading.* Construction and Building Materials, 2026. **506**: p. 144814.
63. Chen, Q.-J., et al., *Dynamic performance of precast concrete columns with pressed sleeve connections under horizontal impact loads.* Engineering Structures, 2026. **346**: p. 121707.
64. Cao, Q., S.-F. Wei, and Z.J. Ma, *Experimental and Analytical Study on Concrete Beams Reinforced with Hybrid Reinforcement under Static and Impact Loads.* Journal of Structural Engineering, 2026. **152**(4): p. 04026007.
65. Sienkiewicz, M., et al., *Environmentally friendly polymer-rubber composites obtained from waste tyres: A review.* Journal of cleaner production, 2017. **147**: p. 560–571.
66. Clemente, P., et al., *Effectiveness of HDRB isolation systems under low energy earthquakes.* Soil Dynamics and Earthquake Engineering, 2019. **118**: p. 207–220.
67. Meng, W., et al., *Experimental and numerical study of a novel slope-type sliding isolation system for seismic protection of electrical equipment.* Soil Dynamics and Earthquake Engineering, 2026. **200**: p. 109919.

Statements and Declarations

Funding

The authors declare that no funds or other support were received during the preparation of this manuscript.

Competing Interests

The authors have no relevant financial or non-financial interests to disclose.

Author Contributions

Syed Abbas Gillani & Majid Ali: Conceptualization, Methodology, Visualization. Syed Abbas Gillani, Ahmad Ibrahim Alam & Muhammad Ali Haider: Experimental Testing. Syed Abbas Gillani: Writing-original draft. Majid Ali: Supervision, Data curation, Writing-review.